



UPPSALA  
UNIVERSITET

*Digital Comprehensive Summaries of Uppsala Dissertations  
from the Faculty of Medicine 1866*

# Ex‘PLA’ining the progression of pathological proteins in Alzheimer’s and Parkinson’s diseases

*see(d)ing is believing*

ANISH BEHERE



ACTA  
UNIVERSITATIS  
UPSALIENSIS  
UPPSALA  
2022

ISSN 1651-6206  
ISBN 978-91-513-1591-1  
URN urn:nbn:se:uu:diva-482999

Dissertation presented at Uppsala University to be publicly examined in Rudbecksalen, Rudbecklaboratoriet, Dag Hammarskjölds Väg 20, 752 37, Uppsala, Friday, 14 October 2022 at 09:15 for the degree of Doctor of Philosophy (Faculty of Medicine). The examination will be conducted in English. Faculty examiner: Associate Professor Hilal Lashuel (École Polytechnique Fédérale de Lausanne, Switzerland).

### Abstract

Behere, A. 2022. Ex'PLA'ining the progression of pathological proteins in Alzheimer's and Parkinson's diseases. see(d)ing is believing. *Digital Comprehensive Summaries of Uppsala Dissertations from the Faculty of Medicine* 1866. 77 pp. Uppsala: Acta Universitatis Upsaliensis. ISBN 978-91-513-1591-1.

Alzheimer's disease (AD) and Parkinson's disease (PD) are the two most common forms of neurodegenerative disorders affecting approximately 50 million people worldwide. The underlying neuropathological processes leading to AD and PD share many similarities, i.e. aberrant protein aggregation of tau and alpha-synuclein ( $\alpha$ Syn) in the brain. Monitoring tau and  $\alpha$ Syn aggregation is challenging, due to morphological heterogeneity of the aggregating species and problems in preserving the antigen conformation *ex vivo*.

In paper-I, we validated the usefulness of proximity ligation assay (PLA), a technique that enabled us to visualize previously undetected early  $\alpha$ Syn pathology in the A30P-tg mouse model of PD. We observed an age-progressive increase in the levels of phosphorylated  $\alpha$ Syn (pSyn<sup>S129</sup>) and the compactness of aggregates in the brain. Although loss of dopaminergic neurons was not found, a subtle dysregulation of other catecholamines was recorded in the older mice.

In paper-II, we revealed a wide distribution of pSyn<sup>S129</sup> aggregates in alpha-synucleinopathy-patient brains. By using a PLA setup with certain antibody pair combinations on brain sections, we observed unique staining patterns, which could not be visualized using regular immunohistochemistry (IHC). In A30P-tg mice, the morphological pattern of the PLA signals indicated an intracellular shift of pSyn<sup>S129</sup> from the periphery towards the neuronal soma.

In Paper-III, we demonstrated that *multiplex* pTau<sup>S202,T205</sup>-pTau<sup>T231</sup>, *singleplex* pTau<sup>T231</sup> and *singleplex* pSyn<sup>S129</sup> PLAs can recognize an extensive tau and  $\alpha$ Syn pathology compared to regular IHC. We found that using our PLA approach we could differentiate between pTau<sup>S202,T205</sup> and pTau<sup>T231</sup> pathology in AD brains, whereas IHC could not. Similarly, in the PD brain, *singleplex* pSyn<sup>S129</sup> PLA detected novel structures, i.e. apparent thick intercellular tunnelling nanotubes and early aggregates; whereas pSyn<sup>S129</sup> IHC was limited to the detection of mature pathology. Lastly, we demonstrated that our *multiplex* PLA approach detected co-aggregates of pSyn<sup>S129</sup>-pTau.

In Paper-IV, in an  $\alpha$ Syn seeding mouse model we observed pSyn<sup>S129</sup> immunoreactivity close to the striatal injection site one day post-injection (dpi). Intriguingly, this type of staining disappeared with the concurrent formation of peri-nuclear pSyn<sup>S129</sup> inclusions in specific brain regions after 14 dpi. In parallel, astrocytic activation prior to pSyn<sup>S129</sup> inclusion formation was observed.

In conclusion, we have developed several novel PLAs that detect both tau and  $\alpha$ Syn pathology with a higher *ex vivo* sensitivity and specificity than currently used immunostaining methods. This thesis work provides valuable insights that potentially could be used for the development of future biomarkers for tauopathies and synucleinopathies.

**Keywords:** Alpha synuclein, Tau, Proteoforms, Phosphorylation, Oligomers, Proximity Ligation Assay, sensitive detection of pathology, Alzheimer's disease, Parkinson's disease, pS129, pS202 pT205, pT231, PFFs

*Anish Behere, Department of Public Health and Caring Sciences, Geriatrics, Box 609, Uppsala University, SE-75125 Uppsala, Sweden.*

© Anish Behere 2022

ISSN 1651-6206

ISBN 978-91-513-1591-1

URN urn:nbn:se:uu:diva-482999 (<http://urn.kb.se/resolve?urn=urn:nbn:se:uu:diva-482999>)

*“ The answers you get depend  
on the questions you ask.”*  
–Thomas Kuhn



# List of Papers

This thesis is based on the following papers, which are referred to in the text by their Roman numerals.

- I. **Behere, A.**, Thörnqvist, P. O., Winberg, S., Ingelsson, M., Bergström, J., & Ekmark-Lewén, S. (2021). Visualization of early oligomeric  $\alpha$ -synuclein pathology and its impact on the dopaminergic system in the (Thy-1)-h[A30P] $\alpha$ -syn transgenic mouse model. *Journal of Neuroscience Research*, 99(10):2525-2539.
- II. **Behere, A.**, Ingelsson, M., Ekmark-Lewén, S., & Bergström, J. A proximity ligation assay recognizing phosphorylated  $\alpha$ -syn reveals previously undetected  $\alpha$ -syn pathology in the brains of synucleinopathy patients and mouse model. *Submitted*.
- III. **Behere, A.**, Ingelsson, M., Erlandsson, A., & Bergström, J. Novel visualization of phosphorylated tau and alpha-synuclein aggregates in the Alzheimer's disease and Parkinson's disease brain. *Submitted*.
- IV. **Behere, A.**, Hårrskog, E., Södergren, M., Ingelsson, M., Ekmark-Lewén, S., & Bergström, J. Alpha synuclein pre-formed fibrils trigger astrocytic activation prior to intra-neuronal deposition in a seeding mouse model of Parkinson's disease. *Manuscript*.

Reprints were made with permission from the respective publishers.

## Additional Publication

- I. Ekmark-Lewén, S., Lindström, V., Gumucio, A., Ihse, E., **Behere, A.**, Kahle, P. J., Nordström, E., Eriksson, M., Erlands-son, A., Bergström, J., & Ingelsson, M. (2018). Early fine motor impairment and behavioral dysfunction in (Thy-1)-h[A30P] alpha-synuclein mice. *Brain and Behavior*, 8(3): e00915.

# Contents

Introduction.....	11
Protein folding.....	11
Protein misfolding.....	12
Protein misfolding diseases.....	13
Alzheimer's disease.....	15
Parkinson's disease.....	16
Tau.....	17
Structure and expression.....	17
Physiological role.....	18
Tau aggregation and hyper-phosphorylation.....	18
Propagation of pathological tau.....	20
Neuropathological diversity.....	21
Alpha-synuclein.....	21
Structure and expression.....	21
Synaptic role.....	22
Role in neurotransmitter release.....	23
Alpha-synuclein and dopamine.....	24
Aggregation of alpha-synuclein.....	24
Oligomers.....	25
Fibrils and strains.....	26
Small aggregates & proteinase K.....	26
Lewy bodies.....	27
Post-translational modification (phosphorylation).....	27
Propagation of pathology.....	28
Neuroinflammation.....	29
Reactive microgliosis.....	29
Role of astrocytes.....	30
Peripheral immune activation.....	30
Aims.....	32
Methodological considerations.....	33
Ethical statement.....	33
Synthetic alpha-synuclein preparations.....	33
Animal models.....	34
Surgical procedures.....	35

Tissue selection and preparations .....	36
Choice of antibodies .....	37
Immunohistochemistry .....	38
Proximity ligation assay .....	39
ELISA .....	41
Immunoblotting .....	42
HPLC .....	43
Microscopy .....	43
Multivariate statistical analysis .....	45
Summary of the investigations .....	46
Paper I .....	46
Paper II .....	49
Paper III .....	50
Paper IV .....	52
Reflections and future perspectives .....	54
Populärvetenskaplig sammanfattning .....	55
सारांश   (sammanfattning på Marathi) .....	57
Acknowledgements .....	59
References: .....	63

# Abbreviations

5-HIAA	5-hydroxyindole-3-acetic acid
5-HT	serotonin
aa	amino acid
AAV	adeno-associated virus
$\alpha$ -syn	alpha-synuclein
AD	Alzheimer's disease
APC	antigen presenting cell
BBB	blood brain barrier
CAA	cerebral amyloid angiopathy
CERAD	Consortium to Establish Registry of Alzheimer's disease
CNS	central nervous system
CSF	cerebrospinal fluid
DA	dopamine
DAT	dopamine transporter
DLB	dementia with Lewy bodies
dpi	days post injection
ELISA	enzyme linked immunosorbent assay
EVs	extracellular vesicles
FFPE	formalin-fixed paraffin-embedded
GCI	glial cytoplasmic inclusion
GFAP	glial fibrillary acidic protein
HPLC	high performance liquid chromatography
IHC	immunohistochemistry
KO	knockout
LB	Lewy bodies
LN	Lewy neurites
MAPT	microtubule associated protein tau
MBD	microtubule binding domain
MHC II	major histocompatibility complex II
MSA	multiple system atrophy
NAC	non-amyloid component
NDDs	neurodegenerative diseases
NFTs	neurofibrillary tangles
NP	neuritic plaque
NT	neuritic thread

PAGE	polyacrylamide gel electrophoresis
PET	positron emission tomography
PFFs	pre-formed fibrils
PK	proteinase K (Keratin)
PD	Parkinson's disease
PDD	Parkinson's disease dementia
PLA	proximity ligation assay
PTM	post-translational modification
RCA	rolling circle amplification
ROI	region of interest
ROS	reactive oxygen species
SNARE	soluble N-ethylmaleimide-sensitive factor attachment protein receptor
SNpc	<i>substantia nigra pars compacta</i>
SV	synaptic vesicle
TANC	tau-associated neuritic cluster
TEM	transmission electron microscopy
tg	transgenic
TH	tyrosine hydroxylase
TNT	tunneling nanotube
TLR	toll-like receptor
VAMP-2	vesicle-associated membrane protein 2
VMAT2	vesicular monoamine transporter 2
VTA	ventral tegmental area
WB	western blot

# Introduction

Proteins are the building blocks of our body; without them, we would not function. The proteins are thus the basic structural units of all cellular life forms. The word ‘protein’ has been derived from Greek *proteios*, which means “the first” or “the foremost”. All proteins consist of the same starting material, which is amino acids (aa). As evident from its name, every single aa contains a backbone with an ‘amine group’ and a ‘carboxyl group’. These aa are coupled to each other with a ‘peptide bond’ that consists of one carboxyl group, attached to the amine group of an adjacent aa. Different functional groups are attached to the carbon backbone of aa. This explains how there can be up to 21 different naturally occurring and potentially many more aa structures with diverse biochemical properties. Through a combination of these 21 aa units, each protein exhibits a unique and specific sequence, consequently achieving an array of biochemical functionalities that range from being parts of a rigid fibrous connective tissue to function as highly dynamic enzymes in the human body.

The vast complexity and richness of proteins lie far beyond the linear aa sequence defined by the genetic code. The combination of genetic variation, alternative splicing and post-translational modifications (discussed later in this section) leads to a rich variety in structure, biological function and sub-cellular localization of proteins. This complexity of proteins is accurately captured by the more inclusive, relatively new, term ‘*proteoform*’,<sup>1-3</sup>. In this thesis, I have utilized the word ‘proteoform’ in this context whenever applicable.

## Protein folding

All native proteins exist as uniquely folded polypeptide aa chains displaying three-dimensional structures according to their aa sequence<sup>4</sup>. They adopt the appropriate 3D structure with a minimal energy configuration with their thermodynamically most stable conformation under physiological conditions. Cyrus Levinthal, in his thought experiment, noted that a protein of an average size has a possibility to attend  $3^{300}$  different conformations and that, hypothetically, the time required to attend the most stable correct conformation in a

sequential fashion would be astronomical<sup>5</sup>. Therefore, he postulated a paradox, suggesting that protein folding is governed under strict thermodynamic control and follows a funnel like energy landscape model to achieve its minimal energy conformation<sup>5-7</sup>. The funnel landscape allows the folding proteins a minimal space to explore and thereby forcing them to adopt minimal energy conformation quickly, through local amino acid interactions<sup>8</sup>. A majority of protein folding takes place within a few milliseconds to minutes<sup>9</sup>. This process is complex and tightly regulated, as protein folding takes place in a crowded cytoplasmic solution with an approximate macromolecular concentration up to 400 g/L<sup>10,11</sup>. Interestingly, other specialized proteins in the cytoplasm that are known as molecular chaperones help proteins to fold correctly<sup>12</sup>. Chaperones guide unstable proteins to fold properly by shielding their exposed hydrophobic aa residues from other hydrophobic aa residues and giving them proper room to fold correctly<sup>13</sup>. Despite the help from chaperones, proteins can misfold; however, these proteins are recognized by the quality control machinery of the cell and are tagged for degradation<sup>14</sup>.

## Protein misfolding

Protein misfolding is a phenomenon that can occur spontaneously when a protein escapes its correct folding pathway from the proposed energy minimizing funnel model<sup>15</sup>. In their native state, most of the functional proteins predominantly exhibit a right-handed spiral coiled loop or an  $\alpha$ -helical structure. It has been noted that when an abnormal conformation change occurs, proteins acquire another structural motif that is known as a  $\beta$ -sheet. However, some of the functional proteins in their native state also exist with  $\beta$ -sheet motifs. Interestingly, the conversion of an  $\alpha$ -helix structure into a  $\beta$ -sheet structure takes place via a partially folded transitional intermediate conformation that is believed to promote aggregation and lead to formation of 'amyloid'<sup>16</sup>. This type of conformational change event can take place randomly or more frequently for certain proteins that have repetitive aa motifs, *e.g.*, polyglutamine in Huntington's disease<sup>17</sup>. In some cases, when a protein adopts a 'toxic' misfolded configuration, it will most likely interact with the other units of native state proteins and promote their configuration to a 'toxic state' via a self-replicating template-amplifying loop. An example of such an infectious self-replicating protein is the prion protein<sup>18</sup>. The figure below describes various possible conformations a protein can attain after its synthesis (**Fig. 1**).

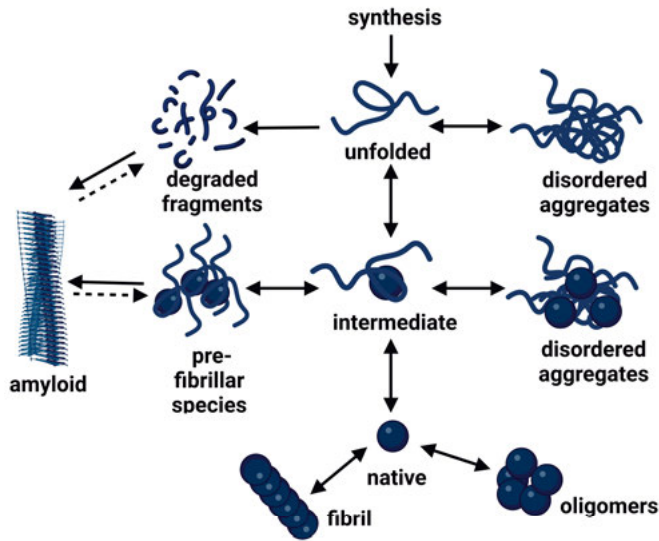


**Figure 1: Conformations of protein in folding and misfolding.** An overview of possible protein conformation states after its synthesis. Image adapted from Dobson 2003<sup>15</sup>.

## Protein misfolding diseases

Protein misfolding diseases, or proteinopathies, are a group of diseases that involve abnormal accumulation of proteins within cells or tissue parenchyma. These diseases are a direct and indirect result of dyshomeostasis of protein synthesis, folding and/or clearance and are, as expected, prevalent in an aging population. Protein aggregation can be triggered by random events, hyperphosphorylation, prion-like self-conversion or by a genetic mutation that might make the protein less stable. Furthermore, genetic mutations responsible for increasing unregulated intracellular concentration of proteins, or imbalances in degradation pathways in proteasome and/or the autophagy machinery, promote amyloid formation<sup>16</sup>. In certain proteinopathies, such as systemic amyloidosis, the amount of aggregates is so large that kilograms of amyloid can be found in the affected organs<sup>19</sup>. However, in some of the proteinopathies of the central nervous system (CNS), the amount of aggregates is so minuscule that they are difficult to detect with currently available biochemical techniques.

In my thesis work, I have focused on detecting the protein aggregates found in Alzheimer's disease and alpha-synucleinopathies, all proteinopathies of the CNS.

## **Amyloidoses**

Amyloidoses of the brain include disorders such as Alzheimer's disease (AD), familial British dementia and familial Danish dementia. All three diseases exhibit neuropathological features, such as intra-parenchymal amyloid plaques or amyloid deposits, cerebral amyloid angiopathy (CAA) and intracellular neurofibrillary tangles (NFTs)<sup>20</sup>. The amyloid cascade hypothesis describes that A $\beta$  (in case of AD)<sup>21</sup> is central to the aetiology and causes downstream events such as formation of NFTs, cell death, vascular damage and dementia. Autosomal dominant mutations identified in the amyloid precursor protein (*APP*), presenilin-1 (*PSEN1*) and presenilin-2 (*PSEN2*) genes result in altered biochemical properties or expression levels of A $\beta$ <sup>22</sup>. As for sporadic AD, the most common genetic risk factor is the *APOE* $\epsilon$ 4 polymorphism, which is believed to affect the clearance of A $\beta$ <sup>23</sup>.

## **Tauopathies**

Tauopathies are a group of brain disorders that involves abnormal depositions of the tau protein, predominantly in neurons but also in glial cells and which manifest in dementia and/or Parkinson-like motor symptoms (Parkinsonism)<sup>24</sup>. Alzheimer's disease is considered both an amyloidosis and a tauopathy, as AD brains also show presence of intra-neuronal NFTs containing aggregated and hyper-phosphorylated tau protein<sup>25</sup>. Furthermore, the mutations in the microtubule associated protein tau gene (*MAPT*) give rise to a form of frontotemporal dementia, which shares many neuropathological features with AD, such as presence of NFTs<sup>26</sup>. Other tauopathies include progressive supranuclear palsy, Pick's disease, corticobasal degeneration, which all manifest into different clinical presentations based on the biochemical profile of tau aggregates, the affected neuronal sub-population and the observed neuro-anatomical location.

## **Alpha-synucleinopathies**

Alpha-synucleinopathies, are the group of neurodegenerative disorders (NDDs) that involve abnormal accumulation of insoluble and fibrillar forms of alpha-synuclein ( $\alpha$ -syn) aggregates in neuronal or glial cells<sup>27,28</sup>. The most common alpha-synucleinopathies are Parkinson's disease (PD), dementia with Lewy body (DLB) and multiple system atrophy (MSA). Both PD and DLB share the histopathological hallmark of Lewy bodies (LBs) and Lewy neurites (LNs), which are intra neuronal inclusions of fibrillar  $\alpha$ -syn<sup>29</sup>, and are collectively termed as Lewy pathologies.

Dementia with Lewy bodies has been reported as the second most prevalent type of dementia after AD and represents approximately 15% cases of all dementia cases<sup>30</sup>. It displays cardinal symptoms such as fluctuations in cogni-

tion, visual hallucinations, and Parkinsonism with combined cortical or sub-cortical dementia. Parkinson's disease dementia (PDD) shares many neuropathological similarities with DLB, except some morphological differences; for example, DLB has a higher load of A $\beta$  in striatum, cortex and amygdala compared to PDD cases<sup>31</sup>. Clinically, these diseases are differentiated by the "one year rule" that is utilized to diagnose DLB, if the cognitive symptoms start within one year after the onset of motor symptoms. If they start later, it is classified as PDD. Furthermore, the PDD cases display more pronounced parkinsonism symptoms in addition to cognitive impairments, whereas DLB symptoms predominantly include visual hallucinations and psychosis<sup>32</sup>.

Multiple system atrophy is characterized by inclusions of fibrillar  $\alpha$ -syn in oligodendrocytes and are termed glial cytoplasmic inclusions (GCIs) or Papp-Lantos bodies<sup>33,34</sup>. It is a rare adult onset neurodegenerative disorder, that can be characterized by progressive autonomic failure, cerebellar ataxia, parkinsonism and pyramidal symptoms in different combinations<sup>35</sup>. Multiple system atrophy affects different neuronal pathways, including striato-nigral, olivopontocerebellar pathways as well as the autonomic nervous system. Furthermore, MSA is clinically sub-classified as 'MSA-P' (Parkinsonism predominant) and 'MSA-C' (cerebellar dysfunction predominant).

## Alzheimer's disease

Alzheimer's disease is the most common form of dementia, representing 60-70% of total dementia cases globally. Currently, dementia is the seventh leading cause of death among the world population<sup>36</sup> and at present, 55 million people suffer from dementia and over 60% of dementia patients live in low- and middle-income countries<sup>36</sup>. Furthermore, dementia affects women disproportionately and 65% of total deaths due to dementia are women<sup>36</sup>. The projected number of people suffering from dementia is expected to have tripled by 2050 and it is considered one of our biggest global public health challenges.

Alzheimer's disease was first described by Dr. Alois Alzheimer, in 1906 when he examined the autopsied brain of his patient Auguste Deter<sup>37</sup>. In her cerebral cortex he observed an abundance of amyloid plaques surrounded by glial cells and neurofibrillary tangles, which are today known as the neuropathological hallmarks of AD<sup>38</sup>. The classical criteria from National Institute of Aging (NIA) proposed 'ABC' criteria to detect AD-neuropathological change on autopsied brains, where 'A' stands for A $\beta$  plaques detected by immunohistochemistry or Thal score, 'B' stands Braak staging against NFTs and 'C' stands for Consortium to Establish Registry of AD (CERAD) score against neuritic plaques by thioflavin-S staining<sup>39</sup>.

Currently, the differential diagnosis of AD from other dementias is performed according to updated research guidelines from NIA, that is based on their ATN criteria<sup>40</sup>. The letter ‘A’ represents amyloid load detected by either decreased cerebrospinal fluid (CSF) levels of A $\beta$ <sub>42</sub> or A $\beta$  positron emission tomography (PET) imaging. The letter ‘T’ represents tau pathology detected either by tau PET or by increased phosphorylated tau (p-tau) levels in CSF. Whereas the letter ‘N’ represents neurodegeneration detected by brain atrophy on proxy imaging methods, such as magnetic resonance imaging (MRI) and PET with <sup>18</sup>F fluorodeoxyglucose (FDG) or by determining total tau (t-tau) levels in CSF.

The neuropathological changes associated with AD are estimated to begin 20-30 years prior to the clinical onset<sup>41</sup>. Therefore, ongoing research is aimed at identifying accurate biomarkers for the pre-clinical phase of AD. Currently, several plasma and CSF biomarker options are being evaluated that can predict the trajectory of AD, several years prior to its clinical manifestations<sup>42,43</sup>.

At present, there are no disease modifying or curative treatments available for AD. The pharmacological management of AD is based on the use of acetylcholine esterase inhibitors, i.e., donepezil, rivastigmine and galantamine, as well as an NMDA-receptor antagonist, memantine<sup>44</sup>. These drugs have a limited effect on the cognitive and behavioural symptoms of AD. In 2021, aducanumab (Aduhelm<sup>®</sup>) became the first anti-A $\beta$  antibody treatment option available, to prevent progression of AD, in patients in the United States. Although it has shown a promising effect on lowering the A $\beta$  load, the clinical benefits of aducanumab have not been clearly significant<sup>45</sup>. Other antibodies and other pharmacological agents designed with an aim to lower either A $\beta$  or tau pathology in AD patients are currently in clinical trials.

## Parkinson’s disease

Parkinson’s disease is the most common neurological movement disorder, affecting about 7 million people worldwide. The incidence of PD is 1% of the population above age of 60 years<sup>46</sup>. Parkinson’s disease patients exhibit the cardinal motor symptoms resting tremor, bradykinesia, rigidity and gait disturbances<sup>47</sup>. These classical motor symptoms of PD are attributed to the depletion of dopamine levels in the striatum, due to a significant loss of dopaminergic neurons of *substantia nigra pars compacta* (SNpc).

Apart from a major loss of dopaminergic neurons, a loss of selective neuronal subpopulations, such as serotonergic neurons of raphe nuclei, noradrenergic neurons of locus coeruleus, and cholinergic neurons of dorsal motor nucleus of vagus, pendunculopontine nucleus and nucleus basalis of Meynert, have

been reported<sup>48,49,49-51</sup>. Although the reasons behind this site-specific and selective neuronal loss are unclear, one of the major common features displayed by all these neuronal subpopulations is the presence of Lewy body-related pathology<sup>52</sup>. A number of non-motor symptoms, such as anosmia, depression, anxiety, sleep disturbances, autonomic dysfunction are prevalent in PD patients and often result in a poor life-quality<sup>53</sup>.

Usually, non-motor symptoms of PD are present already in the prodromal phase, i.e., prior to clinical onset of classical PD symptoms and have been reported to correlate with brain stem pathology<sup>54</sup>. Current efforts are aimed at identifying suitable biomarker candidates that will predict the trajectory of PD and other synucleinopathies in the prodromal phase. Different seed amplification assays, such as protein misfolding cyclic amplification (PMCA) or real time quaking induced conversion (RT-QuIC), can amplify small amounts of misfolded  $\alpha$ -syn aggregates in CSF and have shown promise as diagnostic tools with a high sensitivity and specificity<sup>55</sup>. Furthermore, the detection of misfolded  $\alpha$ -syn in skin biopsies from PD patients have opened new avenues to use minimally invasive methods to detect PD several year before the clinical onset<sup>56</sup>.

Parkinson's disease can, based on the disease aetiology, be classified as either sporadic or genetic. Several mutations involved in a number of genes, such as the  $\alpha$ -syn protein encoding gene (*SNCA*), *LRRK2*, *Parkin*, *PINK-1*, and *DJ-1* can lead to autosomal dominant or recessive forms of PD<sup>57-61</sup>. However, the proteins encoded by these genes are responsible for normal cellular functions related to synaptic vesicle release, mitochondrial energetics, and to the autophagy or lysosomal degradation machinery<sup>62</sup>. Although no curative treatment for PD is currently available, the use of dopamine precursor L-dopa, dopamine agonists, inhibitors of dopamine catabolizing enzymes, anticholinergic drugs, as well as deep brain stimulation may provide symptomatic relief<sup>63,64</sup>.

## Tau

### Structure and expression

Tau, or tubulin-associated unit, was one of the first microtubule associated protein (MAP) that was discovered and characterized in the late 1970's<sup>65,66</sup>. Almost a decade later, tau was identified as a protein forming a core of NFTs, in the AD brain<sup>67</sup>. The adult human protein tau is expressed by *MAPT*. In human brain, it exists as six different isoforms generated by alternative splicing of exons E2, E3 and E10. These isoforms are of different aa length depending

upon the number of 29 aa inserts near N-terminal: 0N, 1N & 2N; and two different repeat domains, i.e., 3R or 4R near the C-terminal. Thus, the protein can exist as differently sized molecules ranging from the shortest 352 aa long 0N3R tau to the longest 441 aa long 2N4R tau isoforms<sup>68</sup>. Structurally, tau can be divided in two domains based on a chymotrypsin cleavage site at residue aa 197. The N-terminal half is called the ‘projection domain’<sup>69</sup>, which does not bind to microtubules, whereas the C-terminal domain spanning from aa 200-400 is called the ‘assembly domain’<sup>70</sup> that is involved in microtubule (MT) interactions. Natively, tau exists as an ‘intrinsically disordered’ or ‘unfolded’ hydrophilic protein, which makes it functionally highly flexible and mobile<sup>71</sup>. Although being a disordered protein, tau prefers to adopt a ‘paper-clip’ conformation, where N- and C-terminal fold and overlap with repeat domains on top of each other. Due to its flexible nature, it is able to bind and interact with tubulin, to stabilize and promote its assembly into microtubules.

## Physiological role

As discussed briefly above, a majority of tau is located in the brain, especially in neurons. It is present ubiquitously in immature neurons in a phosphorylated form, but becomes axonal and non-phosphorylated during the maturation of adult neurons<sup>72</sup>. In adult neurons, small amounts of tau can be found in the nucleus<sup>73</sup> and dendritic spines<sup>74</sup>. Extra-neuronal tau can be found in oligodendrocytes<sup>75</sup> and muscle fibres<sup>76</sup>. The neuronal tau sorting mechanism is not clearly understood, but tau is selectively transported to axons to perform its normal physiological function. The presence of tau in the neuronal soma is a sign of neurodegeneration associated with disease conditions<sup>77</sup>. Tau has an ability to influence retrograde and anterograde axonal cargo transport, as it can compete with the axonal motor proteins kinesin and dynein by blocking their binding sites on microtubules<sup>78</sup>. Currently, the physiological role of nuclear tau in chromosome stability and cellular transcriptomic, as well as its synaptic role, is under investigation<sup>73,79</sup>.

## Tau aggregation and hyper-phosphorylation

Physiologically, tau is a phospho-protein with a normal degree of phosphorylation of about 2 mol PO<sub>4</sub>/mol of protein. However, the AD associated tau is roughly 4 times (~8 mol PO<sub>4</sub>/mol of protein) excessively hyper-phosphorylated<sup>80</sup>. Abnormally hyper-phosphorylated tau is observed in two types of tau filaments: straight filaments (SFs) and paired helical filaments (PHFs) that form the dense core and fuzzy outer layer of NFTs<sup>81</sup>. Additionally, hyper-phosphorylated tau exists in twisted ribbon filaments in AD brains. The PHFs are in majority, representing about 80%, whereas SFs represent approximately

5% of the NFT pathology in AD<sup>82</sup>. The formation of these three different hyper-phosphorylated tau aggregates associated with AD is a widely researched topic.

The initial hypothesis suggested that hyper-phosphorylation promotes aggregation of tau into pathological PHF conformation associated with AD<sup>67</sup>. It was supported by the observation that phosphorylation occurs prior to formation of NFTs<sup>77</sup>. However, *in vitro* data from other groups suggested that recombinant human tau could lead to formation of PHF-like filaments under suitable conditions, i.e., presence of heparin/polyanions, in absence of phosphorylation<sup>83</sup>. A few years later, it was shown that AD p-tau and recombinant human p-tau could self-assemble faster into PHF-like filaments, even in absence of heparin and other co-factors, under physiological conditions<sup>84</sup>. Collectively, these experiments suggested that although phosphorylation of tau is not pre-required for its aggregation, presence of phosphorylation promotes tau aggregation dramatically.

Furthermore, phosphorylation of tau on certain aa residues, especially in the proline rich microtubule binding domain (MBD), such as S231 and S214 or the repeat domain, such as S262, dramatically reduce affinity of tau to microtubule or promote its detachment<sup>85-87</sup>. This phenomenon leads to the release of phosphorylated tau from the microtubule, which may lead to sequestering of normal tau and other proteins, disrupting their normal function and enhanced assembly into PHFs. Moreover, *in vitro* data indicates that pseudo-phosphorylation of tau at S202, T205 and S396, S404 lead to a rigid paperclip fold structure of tau, which in turn induces pathological conformational changes (which can be detected by the MC-1 antibody) as well as enhanced fibrillation<sup>88</sup>.

Multiple kinase enzymes can phosphorylate tau in a site dependent manner. These kinase enzymes can be classified as proline directed protein kinases (PDPKs) and non-PDPKs<sup>89</sup>. The PDPKs have their phosphorylation sites, serine (S) and threonine (T) aa residues in the proline rich domain. Examples of PDPKs include glycogen synthase kinase 3 (GSK-3), cyclin dependent kinase (cdk5) and other enzymes, such as extracellular signal-regulated kinase (ERK), p38 and c-Jun N-terminal protein kinase (JNK), which belong to the mitogen activated protein (MAP) kinase family. The non-PDPKs target S/T residues in the MBDs, which do not contain adjacent proline residues next to phosphorylation sites. The examples of non-PDPKs include protein kinase A and C (PKA & PKC) as well as Ca<sup>2+</sup>/calmodulin-dependent kinase II (CaMKII). Furthermore, these kinases show a certain overlap between their phosphorylation sites. Different protein phosphatases (PPs), such as PP-1, PP-2A and PP-2B, are able to de-phosphorylate tau *in vitro* as well as *in vivo*<sup>90</sup>.

Over 50 different sites of tau can be phosphorylated in the AD brain<sup>91</sup>. However, some of the phosphorylation sites of tau have a greater pathological importance, as antibodies specifically directed against them, have proven to be useful as biomarkers. These phosphorylation sites include different antibodies directed against, PHF-1 (pS396/pS404)<sup>92</sup>, different AT epitopes<sup>93</sup>, such as AT8 (pS202/T205), AT180 (pT231/pS235), AT270 (pT181), AT100 (pT212/pT214) and 12E8 (pS262)<sup>94</sup>. Currently, the pT181, pT217 and pT231 sites are being investigated as the earliest plasma and/or CSF biomarkers, for determining the preclinical phase of AD<sup>95</sup>. Interestingly, recent *ex vivo* evidence suggests that pT181 and pT205 might be two of the most prominent phosphorylation sites that govern the multisite phosphorylation of the human tau protein<sup>96</sup>. Further research will shed new light on the temporal sequence of tau phosphorylation with respect to pathology and/or neurodegeneration.

## Propagation of pathological tau

Tau is considered to be a prion-like protein, which in a misfolded state has a capacity to serve as a template and promote misfolding of native tau<sup>97</sup>. Prion-like spread of tau is considered as one of the main hypotheses behind the distinct and hierarchical involvement of different neuroanatomical regions, as described by the Braak staging of neuropathology. The Braak staging defines six stages of outward spread of brain pathology based on occurrence of NFTs. The NFTs are observed in transentorhinal cortex or enterorhinal cortex of the medial temporal lobe (Braak I & II), before the pathology slowly progresses to involve hippocampal regions (Braak III & IV), and finally the neocortex (Braak V & VI)<sup>98</sup>.

Different cell and animal model experiments indicate that various tau species, either recombinant or extracted from tauopathy patients, have an ability to seed and spread endogenous tau<sup>99</sup>. The aggregation and/or seeding potential of tau is shown to be dependent upon its isoform (described in review by Wang et al. 2016<sup>100</sup>). Furthermore, the seeding activity is dependent upon different mutations or origins of the tau seed (recombinant or patient-derived). Different post translation modifications, such as truncation and phosphorylation, modulate cellular uptake and play a key role in the spreading and seeding capacity of tau. Recently, tau seeding activity was found to correlate positively with hyper-phosphorylated tau oligomers<sup>101</sup>. Interestingly, in the same study hyper-phosphorylation of tau at S198/S199/S202 (AT8) and S400/T403/S404 (PHF-1) indicated a negative correlation and hyper-phosphorylation at T231/S235 (AT180) and S262 (12E8) a positive correlation to its seeding activity<sup>101</sup>.

Inter-neuronal propagation of pathological tau is hypothesized to occur in a sequential manner, with initial release of pathological tau to the extracellular

space, followed by its uptake by a recipient cell, which in turn accumulates endogenous tau to form intracellular inclusions. The release of tau is proposed to occur by passive leakage of dying neurons or when tau dissociates from ghost tangles<sup>102</sup>. However, some studies describe that the release of physiological tau may take place in absence of neurodegeneration<sup>103,104</sup>. Uptake of tau is mediated by endocytosis or by a trans-synaptic route. A recent paper showed that tau seeds can enter a cell via clathrin-independent endocytosis, escape from the endocytosis pathway, and enter the cytosol to misfold endogenous tau<sup>105</sup>. Tau propagation is a bidirectional process along the length of axons (retrograde and anterograde) and exosome-mediated tau spread is considered as another possible mechanism behind the observed bidirectional propagation<sup>106,107</sup>.

## Neuropathological diversity

As described earlier, tauopathies is an umbrella term that describes different neurodegenerative conditions with inclusions of hyper-phosphorylated tau. The observed neuropathological heterogeneity is a combined product of the disease condition, isoform dominance (i.e., either 3R, 4R or mixed 3R-4R tau) as well as the cell-type and/or brain region involvement. This molecular and neuropathological heterogeneity has resulted in more than 20 distinct tauopathies. Although these conditions are grouped together based on the presence of tau inclusions, the observed neuropathology varies drastically (detailed reviewed in Chung *et al.* 2021<sup>108</sup>). For example, neuronal tau inclusions are subclassified as pre-tangle-NFTs, Pick bodies, grains and ballooned neurons. Astrocytic inclusions are defined by ramified astrocytes, tufted astrocytes, thorn-shaped astrocytes, globular astrocytes, granular fuzzy astrocytes and astrocytic plaque. The oligodendrocytic inclusions are subdivided into coiled bodies, Pick body-like inclusions and globular oligodendrocytic inclusions.

## Alpha-synuclein

### Structure and expression

Alpha-synuclein derives its name from its ‘synaptic’ and ‘nuclear’ localization, when it was first described in Torpedo Ray<sup>109</sup>. It belongs to a highly conserved family of synucleins (together with beta-synuclein [ $\beta$ -syn] and gamma-synuclein [ $\gamma$ -syn])<sup>110</sup>. The  $\alpha$ -syn protein is abundantly expressed in the CNS with a higher expression in neocortex, cerebellum, and hippocampus<sup>111,112</sup>. Additionally, its expression has been observed in glial cells and in peripheral organs such as kidney, liver, heart, blood vessels, skin, muscles and bone marrow<sup>76,113–115</sup>.

Alpha-synuclein is 140 aa long and is encoded by *SNCA*. It exists in three different isoforms through alternative splicing. The major 140 aa long protein is structurally divided into three domains as follows (**Fig. 2**):

- i) N-terminal domain (aa 1-60) that contains seven imperfect repeats of 11 KTKEGV motifs that can adopt  $\alpha$ -helical structure when interacting with phospholipids and lipid membranes<sup>116,117</sup>.
- ii) Hydrophobic non-amyloid component (NAC) core region (aa 61-95) involved in self-assembly and aggregation.
- iii) Acidic C-terminal tail (aa 96-140), where different posttranslational modifications (PTMs) can occur.

Most of the identified point mutations leading to familial forms of PD and DLB lie in the N-terminal region. For example, seven missense point mutations in *SNCA* gene have been identified to cause dominantly inherited forms of either PD or DLB: A30P<sup>118</sup>, E46K<sup>119</sup>, H50Q<sup>120</sup>, G51D<sup>121</sup>, A53T<sup>59</sup>, A53E<sup>122</sup>, A53V<sup>123</sup>. Furthermore, duplications<sup>124</sup> and triplications<sup>125</sup> of the wild type *SNCA* gene can also lead to familial forms of PD with a dominant inheritance. Recently, an E83Q<sup>126</sup> mutation that leads to a familial form of DLB was discovered.

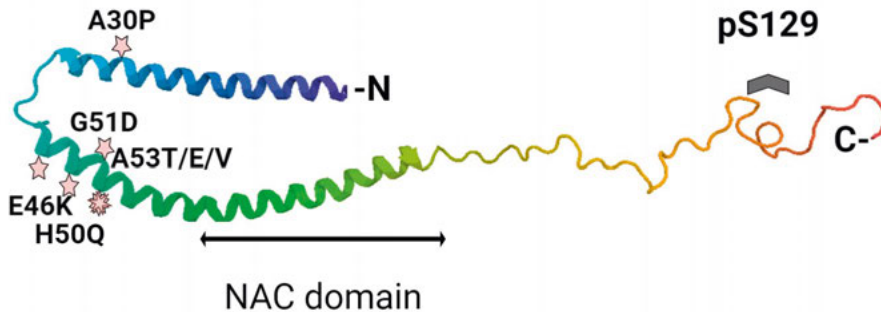


**Figure 2: Structure of alpha-synuclein.** A nuclear magnetic resonance (NMR) predicted structure of micelle bound-human  $\alpha$ -syn expressed by *E. coli*<sup>127</sup>. The N-terminal domain of  $\alpha$ -syn spans from aa 1-60, which interacts with lipid membranes and has 7 missense familial mutations of PD (indicated by stars). The hydrophobic non-amyloid component (NAC) core region spans from aa 61-95 which is involved in self-aggregation of  $\alpha$ -syn. The acidic C-terminal tail spans from aa 96-140, where different post-translational modifications such as phosphorylation (pS129) take place.

## Synaptic role

The physiological role of  $\alpha$ -syn at the synapse remains a largely unanswered question, but its presynaptic localization and ability to interact with lipid membranes advocates for its regulatory role in the synaptic release of neurotrans-

mitters. It acts as a molecular chaperone for soluble N-ethylmaleimide-sensitive factor attachment protein receptor (SNARE) complex<sup>128</sup>. The SNARE complex serves as a molecular zipper enabling the fusion of the synaptic vesicles (SVs) with presynaptic membrane and  $\alpha$ -syn promoting its assembly by binding synaptobrevin-2/VAMP-2 protein of the SNARE complex by its C-terminal and phospholipid membrane of the SVs by its N-terminal<sup>129</sup>. Furthermore, various emerging theories suggest that  $\alpha$ -syn plays a role in synaptic vesicle recycling by modulating the size of readily releasable pool of SVs, its mobilization and endocytosis<sup>130-132</sup>. In addition, physiological  $\alpha$ -syn multimers have been shown to cluster SVs at presynaptic neurons that result in restricted motility and reduced exo/endocytosis of SVs<sup>133</sup>. In the presynaptic chaperone protein cysteine string protein  $\alpha$  (CSP $\alpha$ ) knockout (KO) mice, the precedent neurodegeneration and lethal phenotype is rescued by transgenic (tg) overexpression of  $\alpha$ -syn<sup>134</sup>. This observation suggests that transgenic overexpression of  $\alpha$ -syn can enhance the functionality of SNARE proteins and compensate for the absence of another presynaptic chaperone protein. On the contrary, triple KO mice lacking all three synucleins ( $\alpha$ -,  $\beta$ - and  $\gamma$ -syn) displayed neurological impairments and diminished SNARE protein complex assembly<sup>135</sup>. Furthermore, in a tg mouse line, either expressing truncated human  $\alpha$ -syn (aa 1-120) or human A30P  $\alpha$ -syn, a redistribution of SNARE proteins, reduced dopamine content and SNARE mediated exocytosis were observed, suggesting a toxic gain of function of aggregated  $\alpha$ -syn at the synapse<sup>136</sup>. These studies highlight the essential role of synucleins in maintaining normal functionality of SNARE proteins at the synapse.

## Role in neurotransmitter release

Many studies on cell and animal models have been carried out to address the role of  $\alpha$ -syn in the dopaminergic system. In an animal study on  $\alpha$ -syn KO ( $\alpha$ -syn $^{-/-}$ ) mice, an excess of dopamine (DA) release post-stimulation and a reduced DA content was observed, indicating that  $\alpha$ -syn is a presynaptic negative regulator of DA neurotransmission<sup>137</sup>. Another *in vivo* study on  $\alpha$ - and  $\gamma$ -syn double KO mice concluded that the observed increase in DA release post stimulation was due to an increased release probability of SVs containing DA<sup>138</sup>. Interestingly, human  $\alpha$ -syn overexpression in catecholaminergic cells resulted in reduced exocytosis events by arresting the priming of SVs prior to fusion and release of catecholamines<sup>139</sup>. Another cell study overexpressing different forms of human  $\alpha$ -syn indicated increased cytosolic levels of catecholamines, which was even more pronounced for A30P mutated  $\alpha$ -syn and accounted for the leakage of catecholamines from SVs in the storage pool<sup>140</sup>. A study on rats found that AAV-mediated overexpression of human  $\alpha$ -syn in their nigro-striatal system resulted in a loss of dopamine containing SVs and dopamine release<sup>141</sup>. Taken together, these reports highlight the regulatory role of  $\alpha$ -syn in maintaining normal functionality of dopaminergic neurons *in*

*in vivo* and that altered  $\alpha$ -syn impedes the physiological neurotransmission of DA.

## Alpha-synuclein and dopamine

Dysregulation of tyrosine hydroxylase (TH), vesicular monoamine transporter (VMAT2) and dopamine transporter (DAT) levels/functionality prior to overt loss of dopaminergic neurons in PD have been reported previously<sup>142</sup>. In a dopaminergic cell model, increased  $\alpha$ -syn levels have been shown to decrease TH activity by stabilizing TH in its inactive and non-phosphorylated form and to result in reduced DA production, as TH is a rate-limiting enzyme in DA biosynthesis<sup>143</sup>. Furthermore,  $\alpha$ -syn overexpression increases the activity of protein phosphatase 2A (PP2A), which is responsible for de-phosphorylation of TH, further contributing to a reduction of TH activity<sup>144</sup>. During normal aging, human and primate SN neurons have increased  $\alpha$ -syn levels and decreased TH immunoreactivity, which provides an indirect evidence of the inverse relationship between  $\alpha$ -syn levels and TH activity<sup>145</sup>.

Vesicular monoamine transporter 2 (VMAT2) is responsible for loading the DA in SVs post its synthesis to prevent DA catabolism in the cytosol. However, alterations in level/activity of VMAT2 are considered to be early events that eventually lead to dopaminergic cell death. The overexpression of  $\alpha$ -syn in a dopaminergic cell model resulted in reduced VMAT2 mRNA and protein levels and activity of VMAT2 leading to an induction of higher reactive oxygen species (ROS)<sup>146</sup>. Furthermore, a lower expression of VMAT2 in the SN of PD patients and the presence of VMAT2 in LBs and LNs indicates its association with  $\alpha$ -syn pathology<sup>147</sup>.

Dopamine transporter (DAT) is a presynaptic membrane protein, which is responsible for active uptake and clearance of DA from the synaptic cleft<sup>148</sup>. In cell models and primary dopaminergic neuronal culture, DAT has been shown to be co-immunoprecipitated with  $\alpha$ -syn<sup>149</sup>. In addition,  $\alpha$ -syn has been found to directly bind to DAT<sup>150</sup>. Increased levels of  $\alpha$ -syn are considered to impact negatively on the DAT levels and DAT mediated uptake of DA in cell and animal models<sup>151,152</sup>.

## Aggregation of alpha-synuclein

Natively,  $\alpha$ -syn exists as an intrinsically unfolded random coil monomer under physiological conditions<sup>153</sup>. However, some studies have suggested a 'tetrameric  $\alpha$ -helical  $\alpha$ -syn' as the native structure under physiological conditions<sup>154,155</sup>. Although the notion that native  $\alpha$ -syn exists as an unfolded random

coil monomeric structure is widely accepted in the field<sup>156,157</sup>, increasing evidence is emerging that  $\alpha$ -syn adopts an  $\alpha$ -helical multimeric structure when binding to curved membranes<sup>158,159</sup>. Under aggregation favourable conditions, such as agitation, higher temperature and lower pH,  $\alpha$ -syn undergoes a conformational change resulting in a partially folded intermediate structure<sup>160</sup>. The partially folded intermediates have hydrophobic patches on the surface, which are believed to be essential for continuous self-interaction leading to the formation of oligomers, protofibrils and fibrils with increasing size and hydrophobicity<sup>161</sup>. The  $\alpha$ -syn fibrils are composed of several parallel  $\beta$ -sheet strands that are insoluble<sup>162</sup>. The familial PD associated mutations in  $\alpha$ -syn, as well as some of the environmental conditions such as exposure to pesticide and metal ions, promote  $\alpha$ -syn aggregation and thereby most likely play a significant role in the pathogenesis of certain forms of PD<sup>163</sup>.

## Oligomers

Alpha-synuclein oligomers display a wide range of molecular weights, various degree of  $\beta$ -sheet content and exposed hydrophobicity<sup>164</sup>. They exhibit different structures, such as chain-like, pore-like, spherical, and annular, depending on the environment<sup>165</sup>. A range of  $\alpha$ -syn oligomers exhibit a  $\beta$ -sheet-rich structure and may (on-pathway oligomers) or may not (off-pathway oligomers) eventually form fibrils<sup>166-169</sup>. The A30P and A53T mutations have been shown to increase the rate of oligomerization of  $\alpha$ -syn *in vitro*. Furthermore, *in vitro*  $\alpha$ -syn with the A53T mutation yields annular (10-12 nm in diameter), spherical (~24 nm in diameter) and tubular shaped oligomers, whereas A30P yields annular and spherical oligomers<sup>170</sup>. The distinct biophysical and morphological properties of oligomers are believed to be responsible for phospholipid membrane permeabilization and ROS generation that contribute to cellular toxicity<sup>171</sup>.

Furthermore, the  $\alpha$ -syn oligomers' "gain of toxic function" can affect multiple cellular pathways and exhibit mitochondrial damage<sup>172,173</sup>, endoplasmic reticulum stress<sup>174</sup>, generation of ROS associated membrane damage<sup>175</sup>, induction of abnormal  $\text{Ca}^{2+}$  influx<sup>176</sup>, abnormal microglial activation<sup>177</sup>, autophago-lysosomal dysfunction<sup>178</sup> and synaptic dysfunction<sup>179</sup>. Although it has been technically challenging to visualize  $\alpha$ -syn oligomers, a variety of oligomers have been confirmed with innovative approaches in different cell (e.g., bimolecular fluorescent complementation assay<sup>180</sup>) and animal models<sup>181,182</sup>, in addition to *post mortem* synucleinopathy patient material (e.g., proximity ligation assay PLA<sup>183,184</sup>). Albeit showing toxic cellular effects, the *in vitro* generated  $\alpha$ -syn oligomers do not seem induce the misfolding and recruitment of endogenous  $\alpha$ -syn in animal models<sup>185-187</sup>.

## Fibrils and strains

The aggregation of  $\alpha$ -syn follows a nucleation dependent fibril formation pathway. The addition of  $\alpha$ -syn pre-formed fibrils (PFFs) to monomeric  $\alpha$ -syn solution *in vitro*, omits the primary nucleation of  $\alpha$ -syn aggregation kinetics and triggers elongation of the fibrils directly<sup>188</sup>. Furthermore, the fragmentation of fibrils provides additional surfaces for seeding more  $\alpha$ -syn monomers, thus catalysing the secondary nucleation, which results in enhanced elongation and increased formation of fibrils<sup>163</sup>. In a fashion similar to the *in vitro* experiments, the administration of exogenous PFFs successfully seeded neuronal cells<sup>189</sup>, mice<sup>190</sup> and primates<sup>191,192</sup> resulting in an enhanced aggregation of  $\alpha$ -syn and Lewy body-like pathology *in vivo*.

Interestingly, recombinant  $\alpha$ -syn aggregates have specific conformations and biological activities. Several studies have shown that  $\alpha$ -syn aggregates generated *in vitro* under different salt conditions yield two different types of fibril strains: a cylindrical shaped ‘fibril’ strain and a flat ‘ribbon’ strain. Both of these  $\alpha$ -syn strains have distinct biophysical properties, such as membrane interaction and cellular toxicity<sup>193,194</sup>. Furthermore, *in vitro* sequential passaging of the ‘fibril’ strain leads to formation of a distinct third type of strain that can cross-seed tau into intra-neuronal inclusions<sup>195</sup>. Similar to *in vitro* generated  $\alpha$ -syn strains, intracranial and intramuscular injections in various mouse models with  $\alpha$ -syn aggregates purified from different synucleinopathy brains, produced different strain-specific clinical, pathological and biochemical features<sup>196</sup>.

## Small aggregates & proteinase K

Proteinase K (PK) is a broad spectrum serine protease enzyme that is extensively employed to digest physiological proteins and characterize small misfolded protein aggregates in the prion research field<sup>197</sup>. Digestion with PK can be used to distinguish native/physiological conformations (PK-sensitive) of  $\alpha$ -syn from pathological conformations (PK-resistant) of  $\alpha$ -syn on tissue sections<sup>198</sup>. In addition to PK resistant  $\alpha$ -syn inclusions, PK resistant synaptic  $\alpha$ -syn pathology has been reported in synucleinopathy patient and tg mice brain tissue<sup>199,200</sup>. Furthermore, upon PK treatment of brain homogenates containing  $\alpha$ -syn aggregates, N- and C-terminally truncated smaller  $\alpha$ -syn fragments could be detected following SDS-PAGE<sup>201,202</sup>. The PK resistance property has been attributed to the hydrophobic NAC core of  $\alpha$ -syn, which is implicated in  $\alpha$ -syn aggregation leading to  $\beta$ -sheet conformation<sup>201,202</sup>. Furthermore, altered PK-resistant  $\alpha$ -syn has been detected in the blood of PD patients, opening up new avenues for biomarker strategies<sup>203</sup>.

## Lewy bodies

Lewy bodies (LBs) are the histopathological hallmarks of PD, first described by Fritz Heinrich Lewy in 1912, when he observed the presence of eosinophilic inclusions in the neurons from PD patients<sup>204</sup>. Since then, advancement in histological staining methods, microscopy and computer-assisted visualization methods have helped us to decipher their ultra-structure. Traditionally, LBs were described as dense spherical structure with a core and radiating halo. Subsequently, LBs were found to contain filamentous proteins with lipids and organelles. Based on the filamentous protein arrangement, LBs were classified in two subtypes: classical/brainstem LBs (radiating fibrillar core) and cortical LBs (disorganized fibrils)<sup>205</sup>. The filamentous proteins in LBs were initially thought to be neurofilaments and cytoskeletal proteins, but were later demonstrated to contain fibrillar  $\alpha$ -syn<sup>29</sup>. Although this notion is widely accepted in the field, a recent study claimed that a majority of LBs contains lipids with membranes, organelles and non-fibrillar  $\alpha$ -syn<sup>206</sup>. However, a recent study of LBs describes them as onion skin-like layered structures<sup>207</sup>. In these phosphorylated (pS129) inclusions,  $\alpha$ -syn together with neurofilaments and cytoskeletal proteins form an outer encapsulating structure, containing different truncated  $\alpha$ -syn proteoforms layers with a lipid and/or proteinaceous central core.

## Post-translational modification (phosphorylation)

The post-translational modifications (PTMs) of  $\alpha$ -syn may alter its structure, localization, activity, and degradation. So far, PTMs, such as ubiquitination, nitration, truncation, SUMOylation, acetylation, glycosylation, o-GlcNAcylation and phosphorylation have been described to occur on  $\alpha$ -syn<sup>208</sup>. Phosphorylation at serine 129 (pS129) of  $\alpha$ -syn is one of the major PTMs observed in synucleinopathy patients. A variety of kinases and phosphatases has been suggested to govern phosphorylation and de-phosphorylation of  $\alpha$ -syn *in vivo*. For example, different kinase enzymes, such as G-protein receptor kinases (GRKs), LRRK2 and polo-like kinases (PLKs), could phosphorylate  $\alpha$ -syn *in vitro* and in a cell model<sup>209</sup>. Although pS129-modified  $\alpha$ -syn modulates fibrillation *in vitro* and a large portion (~90%) of  $\alpha$ -syn detected in Lewy bodies is pS129  $\alpha$ -syn<sup>210</sup>, the role of pS129  $\alpha$ -syn in membrane binding, oligomerization, fibril formation and neurotoxicity yet remains largely unclear. However, recent papers indicate that pS129  $\alpha$ -syn, along with C-terminal truncations (CTTs), plays an ultimate role in LB formation<sup>207,211,212</sup>.

## Propagation of pathology

The ascending caudo-rostral pattern of Lewy pathology in different brain regions in PD and DLB cases with progressing disease stages indicates that  $\alpha$ -syn pathology might spread in distinct neuroanatomical pathways in a predictable fashion. Braak and colleagues proposed six stages of Lewy pathology, initiating in olfactory bulb and peripheral vagus nerve, and gradually progressing to brainstem, limbic areas and cortex<sup>213</sup>. Along these lines, a host-to-graft transmission of misfolded  $\alpha$ -syn was proposed as grafted foetal mesencephalic neurons in transplanted PD patients were found to contain  $\alpha$ -syn aggregates after 11-16 years<sup>214</sup>. Additionally, presence of  $\alpha$ -syn aggregates in plasma in PD patients indicates that pathological  $\alpha$ -syn can be released into the extracellular fluid<sup>215</sup>.

The seeding experiments with  $\alpha$ -syn PFF injections indicate that in order to misfold and assemble endogenous  $\alpha$ -syn, the seed must bind to the neuronal / glial cell surface and gain entry into the cytoplasm. Various cell surface receptors and/or various extracellular domains of transmembrane proteins, such as heparin sulfate proteoglycans (HSPGs), lymphocyte activating gene 3 (LAG<sub>3</sub>), neurexin 1 $\beta$ , A $\beta$ -precursor like protein-1 and  $\alpha_3$  subunit of Na<sup>+</sup>/K<sup>+</sup> ATPase are involved in interaction and internalization of fibrillar  $\alpha$ -syn<sup>216-218</sup>. Interestingly, HSPGs-mediated uptake of fibrillar  $\alpha$ -syn by micropinocytosis is highly cell specific to oligodendrocytes, as no uptake can be seen in neither microglia nor astrocytes<sup>219</sup>. Furthermore, the size of the seed (ideal size  $\leq 50$  nm) and PTMs (such as acetylation) plays a role in seed internalization, as demonstrated in several studies<sup>187,220,221</sup>.

Although the PFFs or fibrillar  $\alpha$ -syn is capable of internalizing and seeding *in vivo*, the  $\alpha$ -syn oligomers are found to be the species that spread most efficiently in experimental models<sup>222</sup>. The  $\alpha$ -syn oligomers were shown to transfer via trans-synaptic route mediated by heat shock protein 70 (HSP70). Broadly, the cellular spread of  $\alpha$ -syn oligomers and other aggregation species has been shown to occur via two possible routes: i) exosomes and ii) tunnelling nanotubes (TNTs). Neurons can potentially form and secrete exosomes, i.e. 50-100 nm vesicular cargos containing specific proteins or RNAs that can communicate between cells<sup>223,224</sup>. Different cellular experiments have indicated that the spread of  $\alpha$ -syn oligomers can occur through exosomes<sup>225,226</sup>. Tunnelling nanotubes are cellular protrusions of cytoskeletal proteins that interact and fuse with plasma membranes to send and/or receive cargoes. They can be classified on their size and dimensions as thin TNTs (15-60  $\mu$ m in length, 50-200 nm in diameter) and thick TNTs (30-140  $\mu$ m in length,  $>700$  nm in diameter<sup>227</sup>. The presence of TNT-mediated transfer of  $\alpha$ -syn aggregation species has been visualized by different cell culture experiments in neuronal and glial cells, such as astrocytes<sup>228-231</sup>.

As discussed above, although different cells are involved in the uptake and transfer of  $\alpha$ -syn species, the selective susceptibility to form  $\alpha$ -syn inclusions and vulnerability to degenerate is limited to subpopulation of cells in synucleinopathy patients<sup>232</sup>. Although this central phenomenon is yet a largely unanswered question, two possible hypotheses have been discussed<sup>233</sup>. One line of thought provides an evidence regarding the existing differences in expression level of  $\alpha$ -syn among different cellular sub-populations<sup>234,235</sup>. Meanwhile other experiments describe differential expression levels of protein degradation machinery that may lead to inefficient clearance of  $\alpha$ -syn aggregates and associated vulnerability<sup>236</sup>.

## Neuroinflammation

The inflammation of the brain is generally referred to as neuroinflammation. It involves activation of the different glial cells in the brain and is triggered by pro-inflammatory signalling pathways including the release of different cytokines and chemokines as a response to an insult or a pathogen. Concerning different NDDs, whether neuro-inflammation is a cause or consequence is widely debated. However, ‘chronic neuroinflammation’, together with ‘loss of normal function’ and ‘gain of toxic function’ of the aggregating protein are considered ‘partners in crime’ in the pathogenesis of different NDDs. The human brain inherently lacks immune cells due to presence of blood brain barrier (BBB) and hence glial cells, such as astrocytes and microglia, carry out immune functions in the brain.

## Reactive microgliosis

Microglia are the major type of glial cells in the brain and they are originated from the myeloid cells and perform macrophage-like functions. Microglia are highly mobile cells that can ‘patrol’ the brain, while constantly sensing their surrounding environment. Upon an insult or entry of pathogen in brain, microglia become active, i.e. show changes in their morphology and / or expression levels of surface proteins and secrete pro-inflammatory molecules, a phenomenon termed as ‘reactive microgliosis’<sup>237</sup>. Reactive microgliosis is the first line of the body’s defence mechanism inside the brain. As evident from different experimental models of PD, reactive microgliosis is an early event in PD pathogenesis<sup>238,239</sup>. Furthermore, *post mortem* immunohistochemical analysis and *in vivo* PET imaging from PD patients have indicated presence of reactive microgliosis<sup>240,241</sup>. Now it is clear from multiple lines of studies that misfolded or fibrillar  $\alpha$ -syn initiate a damage-associated molecular pattern (DAMP) that is recognized by microglial pattern recognition receptors, belonging to toll-like receptor family (TLR2 & TLR4)<sup>177,242</sup>. Additionally,  $\alpha$ -syn has been shown to interact with the microglial complement system, which

triggers phagocytosis<sup>243,244</sup>. Thus, microglia play a dual role upon interaction with misfolded  $\alpha$ -syn, *i.e.*, triggering immune activation and promoting its clearance. Paradoxically, when microglial activation is unregulated or abnormally enhanced in disease conditions it might become toxic and contribute to neurodegeneration and pathological protein accumulation. For example, misfolded  $\alpha$ -syn released by neurons interact with microglia, it might trigger caspase-mediated cleavage of  $\alpha$ -syn, leading to its truncation, thereby promoting aggregation and forming a vicious loop<sup>245,246</sup>.

## Role of astrocytes

Astrocytes are stellar-shaped non-neuronal cells that have a neuronal origin. The astrocytes carry out various important functions in the brain, such as forming synapses, nurturing neurons and maintaining the integrity of the BBB. Activation of astrocytes are key features in many pathological conditions of the CNS, including proteinopathies. An increase of GFAP immunoreactivity is considered to be a sensitive marker of activated astrocytes. As discussed earlier in the section above, activation of microglia and elevated pro-inflammatory cytokines in response to misfolded  $\alpha$ -syn might trigger an astrocytic response, due to cross-talk between these two cell types<sup>247</sup>. Reactive astrocytes are classified as A1 and A2 subtypes. A1 astrocytes are known to upregulate pro-inflammatory molecules, whereas A2 astrocytes upregulate neurotrophic molecules. Microglial activation in response to misfolded  $\alpha$ -syn has shown to promote induction of A1 astrocytes via TNF $\alpha$ , IL-1 $\alpha$  and C1q in co-culture experiments<sup>248</sup>. In astrocytes, exposure to misfolded  $\alpha$ -syn led to enhanced secretion of pro-inflammatory cytokines, mitochondrial defects and increased H<sub>2</sub>O<sub>2</sub> production, that are all detrimental factors to neuronal survival<sup>249</sup>. Furthermore, the expression of major histocompatibility complex class II (MHC II) on astrocytic surface in PD brains has suggested that astrocytes may act as antigen presenting cells (APCs) for the brain infiltrating peripheral immune cells that are often reported in the diseased brain<sup>247</sup>.

## Peripheral immune activation

Increasing evidence suggest that PD is a systemic disease and involves accumulation of  $\alpha$ -syn and inflammation in peripheral organs. Furthermore, Borghammer et al. have proposed a hypothesis that  $\alpha$ -syn pathology might also initiate in gut and therefore proposes two sub-types of PD, as 'gut-first' or 'brain-first' PD<sup>250</sup>. Various research groups have been able to provide evidence for this hypothesis in a preclinical setting<sup>251</sup>. Earlier immunohistochemical studies have demonstrated presence of CD4<sup>+</sup> & CD8<sup>+</sup> cells in SNpc of PD brains, indicating that significant infiltration of peripheral T cells occurs during the course of disease<sup>252</sup>. Additionally, presence of infiltrating macrophages

and monocytes have been observed in a PD animal model and *post mortem* PD brain sections<sup>253,254</sup>. Furthermore, elevated amounts of pro-inflammatory cytokines, such as TNF $\alpha$ , IF $\gamma$  in blood, brain and CSF, speaks in favour of MHC II<sup>+</sup>-APC interaction being behind triggering the T cells to mediate this pro-inflammatory response<sup>255</sup>. These lines of evidence speak in favour of T cells playing a key role in PD pathogenesis. Recently, a study demonstrated that peripheral blood mononuclear cells obtained from PD patients, but not healthy controls, could recognize disease associated  $\alpha$ -syn epitopes, such as pS129<sup>256</sup>. The study found that primarily CD4<sup>+</sup>, but also CD8<sup>+</sup>, T cells recognized these epitopes. A follow-up study indicated that the T cell activation is prevalent in the prodromal phase of PD<sup>257</sup>. This has opened up new biomarker avenues for PD patients in clinic. Some studies have found correlations between motor / cognitive performance score and the pro-inflammatory profile of PD patients<sup>255,258</sup>.

# Aims

This thesis work was aimed to explore the pathological protein inclusion formation process in Alzheimer's disease (AD) and Parkinson's disease (PD), by adopting an enhanced *ex vivo* detection technique based on the proximity ligation assay (PLA).

## Specific aims:

- I To visualize and characterize  $\alpha$ -syn oligomers and study their impact on the dopaminergic system in the (Thy-1)-h[A30P]  $\alpha$ -syn tg mouse model of PD.
- II To enhance *ex vivo* detection sensitivity of phosphorylated  $\alpha$ -syn proteoforms in different types of synucleinopathy brain tissue.
- III To investigate the phosphorylated tau and  $\alpha$ -syn proteoforms aggregating in AD and PD brains.
- IV To monitor the temporal evolution of glial and peripheral events prior to inclusion formation, in a PFF seeding mouse model of PD.

# Methodological considerations

## Ethical statement

All animal experimental work included in **papers I, II and IV** was approved by the Uppsala Ethics Committee (ethical permission number: 5.8.18-08038/2018) and the use and housing of animals were performed according to the EU directive 2010/63/EU for animal experiments. All animals were housed at The National Veterinary Institute (Uppsala, Sweden) in open cages on a 12:12 h dark: light cycle, with food and water available *ad libitum*. Brain sections utilized in **paper II** were obtained from the Netherlands brain bank (NBB), Netherlands Institute of Neuroscience, Amsterdam (open access: [www.brainbank.nl](http://www.brainbank.nl) : project number 848). Prof. Irina Alafuzoff kindly provided the brain sections from Uppsala biobank (ethical permission number 2012/494) that were utilized in studies included in **paper III**.

## Synthetic alpha-synuclein preparations

The cryopreserved mouse  $\alpha$ -syn monomers were bought from Proteos Inc., USA (#RP009). The monomers were thawed on ice and then centrifuged. The concentration of  $\alpha$ -syn monomers was determined by measuring the absorbance at 280 nm using a Nano drop. Subsequently, the monomers were diluted with Dulbecco's phosphate-based saline (dPBS without  $\text{Ca}^{2+}$  and  $\text{Mg}^{2+}$ ) to yield the final concentration of 5 mg/ml. The monomers were placed in a safe-seal Eppendorf tube and the cap was sealed using Parafilm. Finally, the Eppendorf tube containing the monomers was placed on a shaker at 1000 RPM in an incubator at 37° C for 7 days.

It is important to perform extensive quality control experiments on the synthetic  $\alpha$ -syn preparation (**Fig. 3**); since it affects the seeding capacity *in vivo*. Sonication was performed upon diluting the yielded PFFs with sterile dPBS at a 1:2 ratio. The working concentration of PFFs was placed on ice and sonicated using the Sonics Vibra cell sonicator with 20% amplitude (1 s off and 1 s on pulses for 60 s). After sonication, the generated PFFs were analysed by transmission electron microscopy (TEM) and their average length was found to be  $31.95 \pm 0.95$  nm, well within the reported optimal range ( $\leq 50$  nm) of the seeding requirements, to result in inclusion formation *in vitro* and *in vivo*.

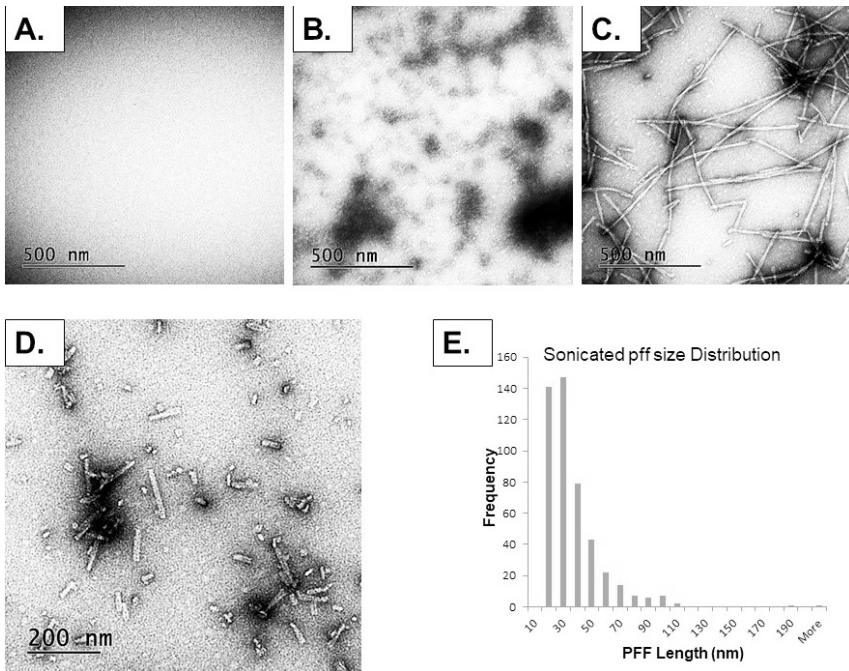


**Figure 3: Transmission electron microscopy (TEM) of synthetic alpha-synuclein preparations.** The figure displaying TEM pictures taken from dPBS (A), monomers (B), pre-formed fibrils (C) and sonicated pre-formed fibrils (D). The quantification of sonicated pre-formed fibrils revealed, their size distribution has been proper (E).

## Animal models

It is said that *‘no model is perfect but some can be useful’* and this statement is true for most of the currently existing animal models of NDDs. An ideal mouse model for PD should recapitulate the loss of dopaminergic neurons in SNpc and age progressive motor impairments, together with Braak stages of LB pathology. However, most of the tg mice models overexpressing human  $\alpha$ -syn display aggregated  $\alpha$ -syn inclusions, but do not mimic the loss of dopaminergic neurons observed in PD/DLB brains. In contrast, the toxin (6-hydroxydopamine, MPTP) based models display loss of dopaminergic neurons, but not the LB pathology<sup>259</sup>.

Some of the most widely used genetic animal models are mice overexpressing tg human  $\alpha$ -syn (wild type, A53T and A30P) under different promoters such as Thy-1, prion, TH, PDGF- $\beta$  etc. Although  $\alpha$ -syn aggregation together with motor and behavioural impairments has been observed in these mouse models, they do not mimic the extensive dopaminergic loss as observed in PD brains<sup>260</sup>. Therefore, after almost a decade of research, different laboratories

have developed and validated newer mouse models of synucleinopathy, which mimic the prion-like spread of  $\alpha$ -syn pathology, neuro-inflammatory response and loss of SNpc dopaminergic neurons<sup>190,261</sup>. Today, mouse models that are extensively used to answer relevant research questions regarding PD and other synucleinopathies are based on: 1) intra-parenchymal injections of pathological  $\alpha$ -syn (PFF seeding model), and 2) viral-vector mediated overexpression of  $\alpha$ -syn<sup>262</sup>.

In our studies in **papers I and II**, we have used the (Thy-1)-h[A30P]  $\alpha$ -syn tg (A30P-tg) mice, which show ~2-fold over-expression of human  $\alpha$ -syn with the A30P mutation and exhibit intra-neuronal  $\alpha$ -syn inclusions. The observed inclusions mimic some features of LB-like pathology, *i.e.*, resistance of  $\alpha$ -syn to PK, Thioflavin S positive staining and phosphorylation at pS129 and the mice also show concomitant motor and behavioural impairments, but without extensive loss of dopaminergic neurons<sup>198</sup>. In **paper IV**, we have used the established PFF seeding mouse model, *i.e.* a unilateral, single intra-striatal injection of msPFF in wt mice. This mouse model was originally developed by Luk et al. 2012 and reportedly showed the appearance at 14+ days post-injection (dpi) of pS129  $\alpha$ -syn inclusions, at 90+ dpi dopamine abnormality, such as TH loss and cell death in SNpc, and at 180+ dpi motor impairments<sup>263</sup>.

## Surgical procedures

We followed the established intra-cranial PFF injection guidelines<sup>220,264,265</sup>. In **paper IV**, we injected 2 months old C57bl/6N male mice with single unilateral intracranial injections of 2  $\mu$ l (corresponding to 5  $\mu$ g)  $\alpha$ -syn in the right dorsal striatum. The mice were carefully monitored for their general health parameters and weight loss for at least 3 days post-surgical procedures.

Prior to injections, the mice were anaesthetized with 4% isoflurane and then fixed on stereotaxic frame, maintaining the anesthesia with 1.5%-2% isoflurane mixed with oxygen throughout the surgery. The body temperature was maintained at 37° C by using a heating pad and a rectal probe was inserted for body-temperature feedback. Carbomer eye gel (Viscotears, Bausch & Lomb) was applied to prevent eye damage due to drying. Local anesthesia with 2.5 mg/ml Marcaine was administered before opening the skin and the incision site was cleaned with iodine solution, followed by 70% ethanol. A hole was drilled in the skull without damaging the dura, using a Kopf high-speed drill.

Material was injected with a Hamilton syringe at a rate of 0.1  $\mu$ l per min into the right dorsal striatum (coordinates: +0.2 mm relative to bregma, 2 mm from the midline) at a depth of 2.6 mm below the dura, with the needle in place for 10 min at target to prevent rapid backflow of its content. After the injection,

the scalp incision was closed using individual sutures and the wound was disinfected with iodine solution. Mice were brought to recovery in a separate cage with an infrared heating lamp until they were self-ambulatory and monitored post-surgery for general health status and weight loss. Painkiller was administered as needed.

At pre-determined time-points post-injection, the mice were anaesthetized with isoflurane before trans-cardial perfusion with 0.9% NaCl solution. Just before starting the perfusion pump, approximately 200  $\mu$ l of blood from aorta was collected via a pipette and immediately transferred to a blood collection tube coated with potassium EDTA and then kept on dry ice. The brains and peripheral organs, such as spleen, liver and 5 mm pieces of duodenum, were removed rapidly and transferred to Falcon tubes with 4% paraformaldehyde.

## Tissue selection and preparations

### **Formalin fixed paraffin embedded tissue**

To preserve the structure, cellular morphology and integrity of epitopes of the tissue, it can be treated with chemical fixatives such as formalin or paraformaldehyde (PFA). This technique of tissue fixation and immobilization is called formalin fixed paraffin embedding (FFPE). It crosslinks proteins and immobilizes cellular components and processes and can be used to store and preserve tissue at room temperature. FFPE sections can be cut using a sledge microtome in various slice thicknesses. Usually, a 5- $\mu$ m thickness is preferred as it corresponds to a single cellular level thick plane in small organs, such as the mouse brain. However, depending upon the tissue rigidity and research requirements the tissue thickness can be adjusted. In **papers I, II, and IV**, we have used 5- $\mu$ m thick FFPE sections; whereas 20- $\mu$ m thick FFPE sections were used in the studies performed in **paper III**.

### **Tissue homogenate preparation**

In **paper I**, the animals used for HPLC experiments were sacrificed by cervical dislocation without perfusion in order to prevent rapid degradation of catecholamines. The obtained brains were snap-frozen using liquid nitrogen and stored at -70 °C before tissue homogenization. The flash frozen brain tissues were weighed and then homogenized in 1 ml ice-cold acetate buffer (pH 5.0) containing 10 ng/ml of 3, 4-dihydroxybenzylamine (DHBA, as internal standard) using a Potter-Elvehjem homogenizer and centrifuged at 21000 xg for 10 min at 4 °C. The supernatant was collected fresh with a pipette and analysed rapidly by loading it in the HPLC cartridges.

Additionally, in **paper I**, a subset of the brain tissue was divided along the midline to separate left from right hemispheres. The right hemispheres were fixed in PFA, as described above. However, the left hemispheres were sub-dissected with a scalpel and a forceps under a bench microscope to separate the midbrain from the non-midbrain tissue fractions (containing olfactory bulb, cortex, hippocampus, cerebellum, brainstem etc. predominantly). The tissues were then homogenized in a PreCellys homogenizer (Bertin Technologies) with 5x w/v of TBS supplemented with Roche's protease cocktail inhibitor (Sigma Aldrich) and an equal volume of 1 % Triton x-100 TBS as extraction buffer. The homogenates were centrifuged at 16000 xg for 1 h at 4 °C, before the supernatant was carefully removed and stored at -70 °C before use.

## Choice of antibodies

Antibodies are useful tools in characterizing the morphological features and assessing pathological levels of  $\alpha$ -syn and tau in tissue material for research and diagnosis of AD and PD. Here, in **papers I-IV**, we have employed a wide array of antibodies to detect  $\alpha$ -syn and tau pathology as seen in table below (**Table 1**).

*Table 1:* An overview of  $\alpha$ -syn and tau antibodies used in this thesis work.

<b>Antibody clones</b>	<b>Host species</b>	<b>Target epitope (aa)</b>	<b>Selectivity claim</b>
<b>MJFR14-6-4-2</b>	Rabbit	n.d.	$\alpha$ -syn filament
<b>5G4</b>	Mouse	46-53	Aggregated $\alpha$ -syn
<b>clone 42</b>	Mouse	91-99	hu / ms $\alpha$ -syn
<b>4B12</b>	Mouse	103-108	hu $\alpha$ -syn
<b>LB509</b>	Mouse	115-122	Pathological $\alpha$ -syn
<b>MJFR1</b>	Rabbit	118-123	hu $\alpha$ -syn
<b>211</b>	Mouse	121-125	hu $\alpha$ -syn
<b>Mab 1338</b>	Mouse	131-140	hu / ms $\alpha$ -syn

<b>Antibody clones</b>	<b>Host species</b>	<b>Target epitope (aa)</b>	<b>Selectivity claim</b>
<b>EP1536Y</b>	Rabbit	120-(pS129)-140	pS129 $\alpha$ -syn
<b>DIR1R</b>	Rabbit	n.d.	pS129 s $\alpha$ -syn
<b>P#64</b>	Mouse	124-(pS129)-134	pS129 $\alpha$ -syn
<b>81A</b>	Mouse	125-(pS129)-133	pS129 $\alpha$ -syn
<b>MN1020</b>	Mouse	AT8 PHF	pS202+pT205 Tau
<b>EPR20390</b>	Rabbit	AT8 synthetic	pS202+pT205 Tau
<b>MN1040</b>	Mouse	AT180 PHF	pT231 Tau
<b>EPR2488</b>	Rabbit	AT180 synthetic	pT231 Tau

## Immunohistochemistry

Immunohistochemistry (IHC) is a broadly used staining method that utilizes antibodies, but today antibody fragments, nanobodies, peptides; affibody molecules are common to target specific epitopes, in order to visualize tissue proteins with a proper contrast. Polyclonal antibodies are a mixture of antibody clones directed at different epitopes of the same protein, whereas monoclonal antibodies bind to a specific epitope of the protein. Therefore, monoclonal antibodies usually display less ‘off-target binding’ and background staining. However, their specificity can be limited due to the conformation of the antigen may cause epitope inaccessibility or to a lower expression of the target protein. Therefore, a step-by-step optimization of the IHC protocol is needed in order to avoid false positive and false negative signals.

Such steps include the reversal of crosslinking (in case of FFPE sections) by antigen retrieval, as crosslinking can mask epitopes and lead to poor binding of the antibody to the target epitope. This can be achieved via treatment with proteolytic enzymes (PK, trypsin etc.), or by providing heat to break the methoxyl bridges between the epitopes, e.g. by boiling in acidic buffer, such as citrate buffer. Other steps include the use of proper buffers and additives to

stabilize the antibodies, permeabilization of the tissue prior to adding antibodies, extensive washing / rinsing with an appropriate concentration of surfactant to remove weakly bound unspecific reactions, etc. Another important step includes blocking non-specific binding by an appropriate buffer, e.g. bovine serum albumin (BSA), normal goat serum (NGS) or a mouse-on mouse (M.O.M.) blocking solution, as usually the antibody preparations contain small traces of serum proteins.

The bound antibody is visualized by a direct or indirect detection method. In a direct detection method, the primary antibody is coupled with a fluorophore or an enzyme, whereas in an indirect detection system, a secondary antibody is coupled to a fluorophore / enzyme that binds to the epitope-reporting antibody. If the target protein is in low abundance, indirect detection is preferred, where the biotinylated secondary antibody's signal can be amplified using enzymatic steps. In bright-field microscopy, an avidin-biotin or streptavidin-biotin-enzyme complex conjugated to a secondary antibody is used for signal amplification that can be visualized by performing enzymatic steps. Either horse-radish peroxidase (HRP) or alkaline phosphatase (AP) is applied, that can precipitate chromogens, Horse-radish peroxidase oxidizes 3,3'-Diaminobenzidine (DAB) to give a red-brown precipitate that can be observed readily. However, tissue samples contain endogenous peroxidase in their cellular compartments that might interfere with the true signal. Thus, it is important to block the endogenous peroxidase activity by using 0.3-3% of H<sub>2</sub>O<sub>2</sub> solution, prior to its chromogenic development.

Sometimes, using fluorophores is a preferred method as it provides with a multiplexing potential, but it also comes with a long-term disadvantage due to instability / fading of fluorophores or a photo-bleaching effect upon long exposure times. Furthermore, immunofluorescent staining of FFPE sections is generally not preferred, as PFA induces auto-fluorescence. After antigen signal development, counter-staining with Mayer's haematoxylin (for bright field microscopy) or 4', 6-diamino-2-phenylindole (DAPI) is performed to stain cell nuclei and visualize tissue architecture. In all the studies (**papers I-IV**), included in this thesis, IHC was performed extensively to examine different tissues and visualize various antigens, such as  $\alpha$ -syn, tau and GFAP.

## Proximity ligation assay

Proximity ligation assay (PLA) is an antibody-based technique that is widely employed to visualize protein-protein interactions at a single molecular level resolution<sup>266</sup>. The PLA probes (antibodies conjugated to oligonucleotides) are employed in order to form a circular DNA, which serve as a template for roll-

ing-circle amplification (RCA). The post-RCA product can be tagged and observed as individual bright puncta under the microscope. The newly developed oligomeric  $\alpha$ -syn PLA (ASO-PLA) is based on using the same monoclonal  $\alpha$ -syn antibody (211) to generate both the PLA probes that enable the visualization  $\alpha$ -syn oligomers<sup>183</sup>. The ASO-PLA has been shown to visualize previously undetected  $\alpha$ -syn pathology on *ex vivo* human brain sections and was found to be 1.6 to 6.5 times more sensitive in detecting  $\alpha$ -syn oligomers than conventional  $\alpha$ -syn immunohistochemistry<sup>183</sup>. It was lauded as the most promising method for specific detection of pathological  $\alpha$ -syn oligomers<sup>267–269</sup>. Furthermore, multiple studies have confirmed the validity of ASO-PLA on human and tg  $\alpha$ -syn mice brain tissue. Furthermore, one group utilized indirect PLA to visualize oligomers/ seeding events occurring between human and mouse  $\alpha$ -syn, in a mouse model<sup>181</sup>. In addition, the presence of  $\alpha$ -syn oligomers in periphery i.e., skin and GI tract biopsy samples opened new avenues for ASO-PLA as a novel biomarker strategy in the synucleinopathy field<sup>270–272</sup>.

This technology is based on use of the Padlock probes. Padlock probes or circularizing oligonucleotides probes are single stranded DNA or linear nucleotides of usually 70-100 or sometimes more nucleotide length, having a target recognition sequence 5'- and 3'- ends. They can be hybridized and brought together by using DNA ligase enzyme. They are bound covalently and cannot be washed away once ligated. In recent years, lot of development in the probe design has led to various new probes that can be utilized to address specific research questions.

**Duolink PLA (Sigma) probes:** These are the primary PLA probes that are employed (direct conjugation of oligonucleotides to 1° antibodies), to reveal the protein interaction, when distance between the proteins is within 30 nm<sup>266</sup>, whereas, secondary PLA probes are employed (direct conjugation of oligonucleotides to 2° antibodies), protein interactions within 40 nm are captured<sup>273</sup>. The primary PLA probes are utilized in **Paper I**, whereas, secondary PLA probes (**Fig. 4**) are utilized in **Paper II, III and IV**.

**ProxHCR probes:** ProxHCR stands for proximal binding hybridization chain reaction that utilizes enzyme free system with specialized kinetically trapped hairpin structured probes that are bound to antibodies that can be amplified exponentially upon activation by an activator oligonucleotide<sup>274</sup>.

**UnFold PLA (NaVinci) probes:** These are the improved version of originally described direct PLA probes with additional enzymatic 'unfolding' step<sup>275</sup>. These modified probes have a hairpin- loop structures (containing uracil moieties) within the circle forming oligonucleotide probe and its complementary template probe. The hairpin- loop structures block the binding of complemen-

tary oligonucleotides to each other prematurely upon their simultaneous introduction to the sample. After, both antibodies (conjugated to UnFold probes) are bound, enzymes called uracil-DNA glycosylase (UNG) and endonuclease IV (EndoIV) are applied to ‘unfold’ the probes, allowing them to remove uracil moieties, in order to get ligated for the following steps. We have utilized the UnFold PLA probes for PLA experiments in **Paper IV**.

**MolBoolean PLA probes:** This is the most recent advancement in PLA technology that can report ‘NOT’ and ‘AND’ Boolean functions of interacting proteins, thus generating signals in three separate channels simultaneously, thereby informing protein interaction within 40 nm in a separate channel and individual proteins that are in the proximity but not interacting in their individual separate channels<sup>273</sup>.

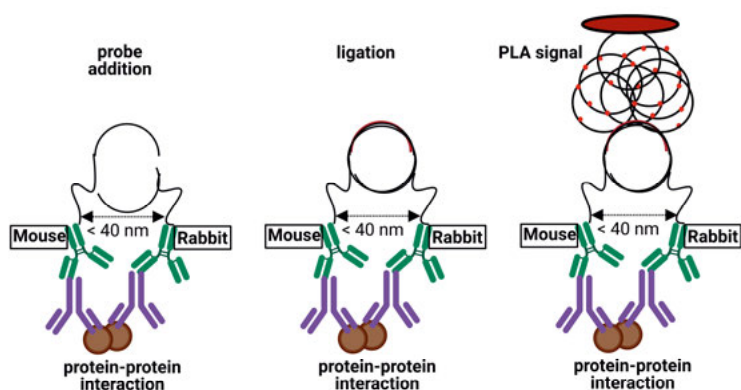


*Figure 4: The principle behind indirect proximity ligation assay (PLA).* The proteins of interest that lie <40 nm apart can be targeted with primary antibodies of different species. The PLA probes (secondary antibodies conjugated to oligonucleotides) are employed in order to form a circular DNA, which serve as a template for rolling-circle amplification (RCA). The post-RCA product is then tagged to be observed as individual puncta under the microscope.

## ELISA

The enzyme-linked immune-sorbent assay (ELISA) is an easy and relatively accurate method to quantify the molar concentration of protein analytes in a solution. It is a widely used immunological detection method to quantify proteins from multiple biological samples in a single experiment. It can be performed in many different ways, by changing the parameters behind the same principle of antibody-antigen binding interaction, i.e., direct, indirect, sandwich and competitive ELISA. It involves the first coating step, where immobilization of antigen / coating (capture) antibody on a solid phase takes place, e.g., 96-well polystyrene microplate. Thereafter, a blocking step limits un-

specific binding interactions. This step is followed by analyte incubation for signal detection. After performing these consecutive steps with in-between washes, a signal measurement is carried out. In **paper I**, we have used a sandwich ELISA to quantify different  $\alpha$ -syn species in mouse brain tissue homogenates. First, an epitope-specific  $\alpha$ -syn antibody was coated on the ELISA plate. After the blocking step, samples and standards were incubated. After this step, a biotinylated antibody targeting the same  $\alpha$ -syn epitope (to detect oligomers) or non-overlapping  $\alpha$ -syn epitopes (to detect total and phosphorylated  $\alpha$ -syn) were added. This was followed by sequential addition of streptavidin conjugated secondary antibody, and HRP for signal amplification. The chromogen development was carried out using 3, 3', 5, 5'-tetramethylbenzidine (TMB) and  $H_2SO_4$  to stop the chromogenic reaction. The absorbance or optical density (OD) values were measured at 450 nm.

**MSD multiplex ELISA:** MSD (Meso Scale Discovery) designs multi-spot panels with multiple pre-coated capture antibodies on an electrode surface per well of 96-well ELISA plate. By utilizing this highly specialized calibrated ELISA plate, one can detect multiple analytes from single- small volume sample. The detection step consists of addition of mixture of antibodies conjugated with electrochemiluminescent (ECL) labels or MSD SULFO TAG. This step completes the ELISA sandwich, after that adding specialized MSD buffer and applying voltage to the electrode-coated MSD plate lead to emission of a light proportional to the concentration of bound SULFO TAG antibodies. This emitted light is measured by the MSD plate-reader to provide a quantitative output on molar concentrations of different analytes. In **Paper IV**, we used the V-plex 10 spot pro-inflammatory panel that can detect IFN- $\gamma$ , IL-1 $\beta$ , IL-2, IL-4, IL-5, IL-6, KC/GRO, IL-10, IL-12p70, and TNF $\alpha$  cytokines in blood samples.

## Immunoblotting

Sodium dodecyl sulphate-poly-acrylamide gel electrophoresis (SDS-PAGE) is an extensively used technique in molecular biology to achieve separation of proteins based on their molecular weight (MW). It involves an initial step, where denaturing of protein (usually boiling the samples together with SDS) is carried out to disrupt the protein's tertiary structure by breaking di-sulphide bonds and thereby unfold it to a linear polypeptide chain. The highly negatively charged SDS binds to the protein backbone in an equal molar ratio to the entire linear peptide chain length. The vertical separation of proteins is achieved via applying an electric potential. The protein migrates from the cathode side towards the anode. The rate of migration is controlled by different combinations of gel polymers to yield different pore sizes, which in turn offer resistance to high MW proteins, while allowing low MW proteins to run

through the gel, thus achieving a protein separation gradient. The separated proteins are then transferred horizontally from the gel onto a membrane and fixed with PFA (usually, in case of  $\alpha$ -syn). The transferred protein can be stained with antibodies. This technique of immunoblotting is termed as ‘western blot (WB)’. In **paper I**, we measured PK resistance to  $\alpha$ -syn aggregates by using WB.

## HPLC

The high-performance liquid chromatography (HPLC) system consists of three main units: the injector, the pump and the detector. The detector sends a signal to a computer, where a software assisted construction of a chromatogram takes place. The pump transports the Mobile Phase to the injector via a fluctuating dampener and guard cell. The injector adds a sample or a standard to the Mobile Phase, which is then pumped through a column that separates different compounds within the sample. In the next step, the sample passes through the cell where different compounds get oxidized by a positive potential, resulting in the generation of an electric current directly proportional to its oxidation potential. The generated electric signal is picked up by the detector and amplified before getting transformed into a chromatogram seen on the computer screen. In **paper I**, we analysed the levels of brain monoamines & their metabolites- norepinephrine (NE), serotonin (5-HT), 5-HT metabolite 5-hydroxyindole-3-acetic acid (5-HIAA), dopamine (DA) and its metabolites dihydroxyphenylacetic acid (DOPAC) and homo-vanillic acid (HVA) by using an HPLC system with electrochemical (EC) detection.

## Microscopy

### **Bright-field microscopy**

Light microscope uses transmitted white light in combination with its lenses to generate a magnified image of a specimen and at the same time, image contrast is achieved by absorption of light by the specimen. Usually, the microscope consists of two lenses: an objective lens (focuses on the placed specimen) and an ocular / eye-piece lens (magnifies the image of the focused specimen). Resolution of a microscope refers to the minimal distance between two points that can be visualized separately. It is based on the Rayleigh’s criterion that describes that the resolution is directly proportional to the wavelength of the passing light, inversely proportional to its numerical aperture. The numerical aperture defines the ability of the objective lens to capture light, which is a product of the refractive index of the medium as well as the angle between

the objective and the specimen. The refractive index is a ratio between velocity of light in a medium / velocity of light in vacuum. Thus, increasing the refractive index by using an oil results in an enhanced resolution. Thus, the oil-immersion method is preferred with lenses with larger numerical aperture, *e.g.* a 63x objective. Usually, the resolution limit of light microscope is around 200 nm but can be affected by the levels of background signal. In all the studies (**papers I-IV**) included in this thesis, bright-field microscopy was extensively used to visualize and capture pictures of the tissue sections.

### **Fluorescence/Fluorophore-based microscopy**

An absorption of light (or photons) by a molecule promotes its electrons to a higher energy state, *i.e.*, the excitation state. The excited electron can return to its ground state by several ways that are described by a Jablonski diagram. When an excited electron undergoes relaxation to its ground state by emission of light, this process is termed as ‘photo-luminance’. Fluorescence is a type of photo-luminance, where the return of the electrons to their ground state occurs without changing the electron spin. A molecule that can adopt a fluorescence state is termed a ‘fluorophore’. Fluorophores are organic aromatic structures that display properties, such as absorption and emission of light at only specific wavelengths. Hence, using a proper combination of fluorophores with non-identical excitation and emission spectra is critical in order to prevent merging of the signals. Fluorescent imaging relies upon its objective lens for both illumination and collection of a reflected fluorescent emission. In order to excite a fluorophore, only lights of certain wavelength are suitable. This can be achieved via a series of in-built filters. These filters allow for the passing of white light from the light source before allowing the remaining light to pass through the objective for focus and magnification. After reaching the specimen, the reflected light again passes through the objectives and the filters before reaching to the eyepiece / attached camera. In **paper IV**, fluorescent microscopy was used to visualize and capture pictures of the tissue sections.

### **Transmission electron microscopy (TEM)**

Transmission electron microscopy (TEM) utilizes the electrons that are transmitted through the specimen creating electron diffraction. It operates via a broad electron beam focused on the mounted sample. The image is acquired by projecting the electrons directly on a charged coupled device (CCD) camera that generates a projected 2D image. Using TEM, a very high, resolution (1Å) can be achieved. However, the electrons are transmitted through the entire thickness of a sample. Hence, the sample needs to be thin (around 100 nm) or in the form of a properly diluted suspension on a grid treated with heavy metal, in order to achieve high electron density for proper image contrast. In **paper IV**, we extensively used TEM to confirm the presence of PFFs or fragmented proteins with or without (for pure monomeric preparations) sonication.

## Multivariate statistical analysis

The multivariate statistical analysis is employed to extract information from large data sets. It uses primarily two different methods: i) principal component analysis (PCA), ii) partial least square (PLS) regression analysis. To reduce data dimensionality and extract the variance between uncorrelated variables systematically, PCA uses 'eigenvectors' to extract information about this variance. The Eigenvectors are the non-zero vectors, which undergo scalar transformation to give only scalar values i.e. eigenvalues. The eigenvalues are orthogonal to each other, thus creating a space to include linear combination of variables and observations. Hence, arranging the observations by largest variation factor and second largest variation factor in an orthogonal spread on 2D space. This orthogonal spread or the data-point overview enables the observer with visual understanding of how two observation are similar, i.e. data points clustered together, share similarities while the points spread far away from each other have opposite properties. Furthermore, in order to understand, in what way the data points are similar or different, one can investigate or superimpose 'loading plot' on the 'score plot' with data points. The loading plot contain information about characteristic properties that strongly influence spread of principal components in 'score plot'. In **Paper II**, we utilized PCA to estimate efficiency of four different antibody-pairing combinations in PLA with different synucleinopathy conditions and multiple staining variables.

# Summary of the investigations

Alpha-synuclein is often referred to as a ‘protein chameleon’ due to its ability to exist in various dynamic conformations under physiological conditions<sup>160</sup>. This property of  $\alpha$ -syn with its ability to exist in multiple conformations adds another layer of complexity while detecting different aggregation species proposed to be occurring during different disease conditions. Alpha-synuclein displays molecular heterogeneity in terms of its aggregation species - dimers, trimers, tetramers, soluble oligomers, kinetically stable oligomers, large oligomers, various type of fibrils<sup>163</sup>. To complicate matters further, different PTMs, particularly phosphorylation and truncations, have been reported to influence different aggregation species and their cellular localization. Naturally, investigating and pinpointing the  $\alpha$ -syn aggregation species responsible for and/or correlating with neurodegeneration or disease stages is a question of high clinical relevance. Currently, the research heavily relies on usage of antibodies raised against different epitopes of  $\alpha$ -syn to target different conformations / aggregation species. However, recently a group of researchers discovered that 16 commercially available and widely employed  $\alpha$ -syn antibodies could not differentiate between  $\alpha$ -syn conformations<sup>276</sup>. This finding highlights the need of an innovative approach to overcome this technical limitation and thereby characterize the aggregation species with a reliable *ex vivo* technique.

## Paper I

### **Optimization of ASO-PLA for *ex vivo* detection of $\alpha$ -syn oligomers and associated pathological changes**

To address the technical limitation of antibodies to accurately determine  $\alpha$ -syn conformation due to the morphological complexity of  $\alpha$ -syn aggregation species, we decided to make use of proximity ligation assay (PLA), together with other available biochemical techniques in an *ex vivo* experimental setup. We chose the (Thy-1) -h [A30P]  $\alpha$ -syn tg (A30P-tg) mouse model, bred and housed in our laboratory, since its pathological profile has been well characterized. After undergoing several trouble-shooting and optimization steps us-

ing the original  $\alpha$ -syn oligomer detection PLA (ASO-PLA) protocol developed by Roberts et al. 2019<sup>277</sup>, we observed an age-dependent characteristic shift of  $\alpha$ -syn oligomers from a punctate to a patchy to a clustered appearance (as seen in **Fig.5**) in brains from A30P-tg mice. Interestingly, in 2 months old mice, the presence of abundant oligomers with a punctate morphological pattern could be detected in the midbrain region. There have been no previous reports indicating the presence of oligomers in such young mice<sup>198,278,279</sup>, while one report has suggested that oligomers cannot be observed until 4 months of age<sup>280</sup>.

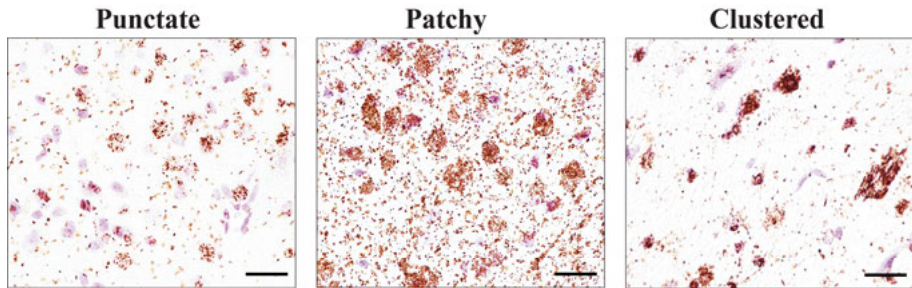


**Figure 5: Patterns of PLA signal.** The characteristic morphological shift of  $\alpha$ -syn oligomers from punctate to patchy to clustered as detected by ASO-PLA in the mid-brain of A30P-tg mice.

### **Comparison of morphological changes observed with ASO-PLA with other biochemical techniques**

Our ASO-PLA experiments thus revealed a previously undetected abundance of  $\alpha$ -syn oligomers in the midbrain of A30P-tg mice, as early as 2 months of age and peaking already at 5 months of age. To assess and validate the *ex vivo* presence of oligomers in midbrain and other regions in these mice, we analysed the sub-dissected midbrain and non-midbrain homogenates with an ELISA specifically developed to detect  $\alpha$ -syn oligomers in cell and tissue lysate<sup>281</sup>. To assess the compactness of the  $\alpha$ -syn aggregation species, we employed western blot (WB) assay on PK treated brain homogenates, as described previously<sup>199</sup>. We showed that 2 months old mice had significantly higher levels of TBS-T soluble (membrane-associated) oligomers, compared to older 11 mo mice. In addition, higher levels of TBS-T soluble total and oligomeric  $\alpha$ -syn were observed in the brain homogenates of 2- and 5-months old mice, compared to 8- and 11- months old mice. Furthermore, we found an increasing trend in PK resistance in 8- and 11-months old mice compared to 2 months old mice (**Fig. 6**). We further validated these findings by performing PK treatment prior to ASO-PLA staining. These experiments indicated that higher PLA signals persist in 5-, 8- and 11-months old mice after PK treat-

ment. Taken together, we interpreted the data that an increase in  $\beta$ -sheet content, morphological compactness, misfolding, hydrophobicity and TBS-T solubility of  $\alpha$ -syn aggregates can be observed over time in this mouse model.

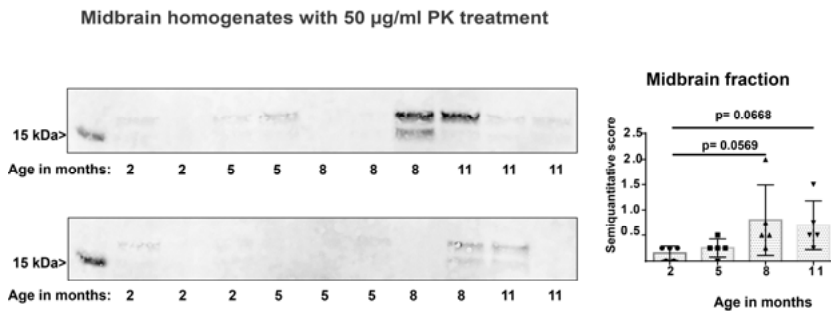


**Figure 6: The western blot assay with PK treatment on midbrain homogenates.** The TBS-T midbrain fractions indicated a trend towards age-progressive enhancement in PK resistant  $\alpha$ -syn species across young vs. middle-aged A30P-tg mice.

### Association of phosphorylation of $\alpha$ -syn with observed biochemical changes

The next question was to assess the association of the observed biochemical changes in these mice with the phosphorylation profile of  $\alpha$ -syn at the serine 129 residue (pSyn<sup>S129</sup>), which is generally considered a marker for its aggregation status *ex vivo*. We observed an age-progressive, linear trend displaying an increased level of pSyn<sup>S129</sup> species, as determined by both ELISA and immunohistochemical analyses. Taken together, these data suggest that pSyn<sup>S129</sup> might be a good *ex vivo* marker of  $\alpha$ -syn aggregation in this mouse model.

### Determining effects of biochemical changes in $\alpha$ -syn on midbrain dopaminergic neurons

Lastly, we sought to identify the molecular mechanisms behind the impaired motor and behavioural phenotype reported in these mice<sup>282</sup>. We investigated the potential link between  $\alpha$ -syn-associated biochemical changes and the functionality of midbrain dopaminergic neurons by analysing the levels of dopamine and its metabolites by HPLC and TH immunoreactivity. However, we did not find any differences in any of the analysed parameters, suggesting that biochemical changes of  $\alpha$ -syn or its aggregation did not appear to significantly alter the functionality of dopaminergic neurons and that the reported motor and behavioural changes therefore might occur due to reasons that are not related to dopamine.

## Paper II

### Optimization and development of PLA to target pSyn<sup>S129</sup> aggregation species across different synucleinopathies

Here, using PLA, we systematically paired four different antibodies targeting different regions of  $\alpha$ -syn (ranging from its N- to C-terminal) with an antibody detecting pS129-  $\alpha$ -syn. We used this experimental setup to visualize pathomorphological features of  $\alpha$ -syn aggregates on *post mortem* brain tissue from PD, DLB and PDD. Furthermore, we sought to visualize sub-regional differences in pSyn<sup>S129</sup> aggregation species in A30P-tg mice with our experimental setup, as this mouse model has been previously reported to contain subtle morphological differences in the sub-regional distribution of pSyn<sup>S129</sup> aggregation species<sup>283</sup>. Additionally, we paired two antibodies targeting the same pS129 residue site, to understand whether this combination enhances *ex vivo* sensitivity and specificity of phosphorylated  $\alpha$ -syn detection (discussed later in this section).

We analysed the morphological staining patterns on the brain tissue sections using PLA with different antibody combinations and compared it to regular immunohistochemistry against the pS129 and four other  $\alpha$ -syn epitopes (**Fig. 7**). We could observe that PLA staining with certain antibody combinations, i.e., LB509 and Syn-1 (clone 42) with PS129 epitope selective antibody, yielded an enhancement in the detection of early cytoplasmic aggregates, in addition to Lewy pathology. However, when the 5G4 antibody was combined with PS129 epitope selective antibody, an enhancement in pathological detection of  $\alpha$ -syn could not be seen. These experiments suggest that certain epitopes are more exposed than others in the  $\alpha$ -syn aggregates, verifying earlier similar findings from the laboratory using polyclonal antibodies raised against synthetic peptides corresponding to short linear  $\alpha$ -syn sequences<sup>284</sup>. Thus, an appropriate choice of antibody combination can enhance the *ex vivo* detection of  $\alpha$ -syn aggregation species. In A30P-tg mice, the morphological pattern of PLA signal indicated an age-progressive, intracellular shift of pSyn<sup>S129</sup> aggregation species from the periphery towards somal compartment in the prefrontal cortex.

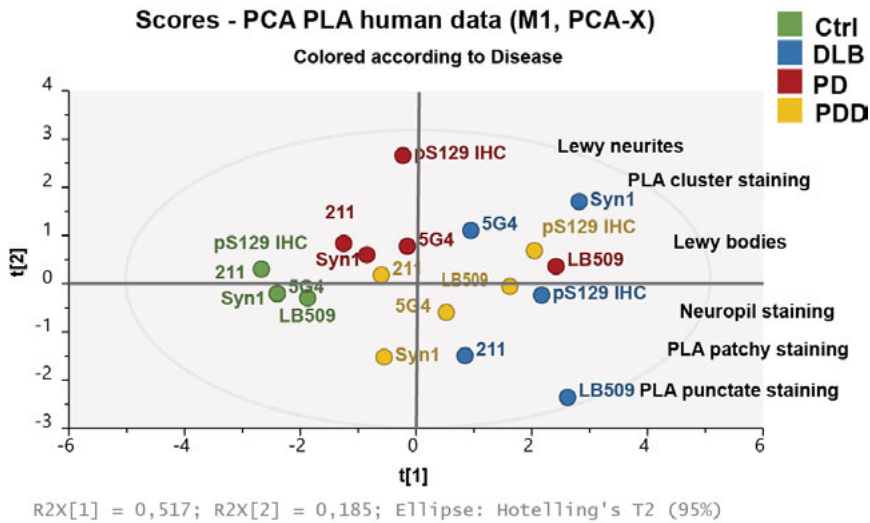
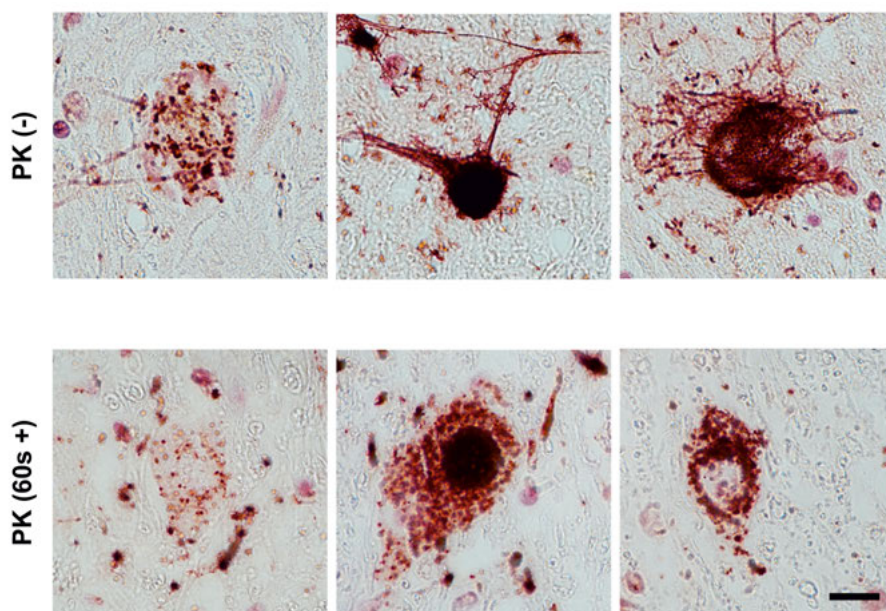


Figure 7: **Antibody pairings in PLA and their morphological staining pattern.** Principal component analysis (PCA) displays the scores of the two-first principal components ( $t[1]$  and  $t[2]$ ) for individual type of staining method used. The control cases (green dots) were mainly positioned to the left side of score plot and thus were separated from synucleinopathy cases (blue, red and yellow dots) seen on the right side of the score plot.

## Paper III

### ***Singleplex* PLA protocol targeting pS129 epitope reveals novel pathological features in the PD brain**

After a series of experiments involving protocol optimization as mentioned in sections above, we observed that by combining two antibodies targeting the same PS129 epitope in a PLA setup, we could improve the detection specificity and sensitivity of  $\alpha$ -syn aggregates. The *singleplex* pSyn<sup>S129</sup> PLA detected novel pathological structures, such as apparent thick intercellular tunnelling nanotubes and pre-Lewy body intracytoplasmic aggregates (**Fig. 8**), whereas pSyn<sup>S129</sup> IHC was limited to the detection of mature Lewy pathology. We performed a series of control experiments to determine the PK resistance of the detected aggregates and their unique morphological features. The detected intracytoplasmic pS129  $\alpha$ -syn aggregates were highly resistant to PK, whereas the pS129 positive staining of apparent tunnelling nanotubes and neurites were PK-labile (**Fig. 7**). This indicates that our *singleplex* pSyn<sup>S129</sup> PLA can detect novel PK-resistant  $\alpha$ -syn oligomers, which are not the same as the PK-labile oligomers observed by other groups using the homotypic 211-antibody based PLA approach<sup>183,184</sup>.



**Figure 8: Novel structures detected by *singleplex* pSyn<sup>S129</sup> PLA.** The *singleplex* pSyn<sup>S129</sup> PLA on PD *substantia nigra* sections revealed novel structures such as, early cytoplasmic aggregates and tunnelling nanotubes. The apparent thick tunnelling nanotubes disappeared after 60 s of PK treatment, but cytoplasmic signal persisted. **Scale bar: 10  $\mu$ m.**

### **Optimization and development of the PLA protocol to target site specific phosphorylation at S202/T205 and T231 residues**

Recently, a paper employing a homotypic tau-5 antibody PLA (i.e., specifically detecting tau oligomers) described that this approach was highly successful in enhancing detection sensitivity of early pathological changes in AD brains<sup>285</sup>. Furthermore, the authors described a sequential pattern of molecular changes in tau pathology that can be detected as follows: tau multimerization (by homotypic tau-5 PLA), followed by IHC against AT180 (pTau<sup>T231</sup>) epitope and lastly IHC against AT8 (pTau<sup>S202/T205</sup>) epitope<sup>285</sup>. However, they did not investigate the homotypic interaction between phosphorylation at S202/T205 and T231 sites of tau by PLA. Therefore, we developed a PLA that could specifically detect homotypic and heterotypic interactions between pTau<sup>S202, T205</sup> and pTau<sup>T231</sup> in AD brains. Our results indicate that *multiplex* pTau<sup>S202, T205</sup>-pTau<sup>T231</sup> and *singleplex* pTau<sup>T231</sup> could enhance detection of tau pathology compared to regular immunohistochemistry (IHC), using either of the pTau<sup>S202, T205</sup>, pTau<sup>T231</sup> antibodies on adjacent brain sections.

### **Phosphorylation at S202/T205 and T231 residues indicate differences with respect to their aggregation state**

Next, we sought to address the discrepancies in the signals visualized by *singleplex* pTau<sup>S202, T205</sup> versus *singleplex* pTau<sup>T231</sup> PLA, when IHC against pTau<sup>S202, T205</sup> or pTau<sup>T231</sup> does not indicate significant differences in their immunoreactivity profile. Therefore, we decided to address this phenomenon by analysing the effect of PK treatment on adjacent sections. We observed, upon PK treatment, that most of the *singleplex* pTau<sup>T231</sup> and *multiplex* PLA pTau<sup>S202, T205</sup>-pTau<sup>T231</sup> signal disappears, whereas *singleplex* pTau<sup>S202, T205</sup> PLA remained unaffected or even showed higher signals. Thereby, we interpret that these discrepancies represent differences in the aggregation status of  $\alpha$ -syn. We hypothesize that PK-labile homotypic pTau<sup>T231</sup> interactions represent non-compact and/or non-fibrillar and diffuse aggregates, while the homotypic pTau<sup>S202, T205</sup> interactions represent a compact, fibrillar and denser type of aggregates.

### **Proof of concept: detection of pTau-pSyn hybrid oligomers**

Lastly, we could demonstrate that our novel *multiplex* PLA approach also can be applied to detect co-aggregates of pSyn<sup>S129</sup>-pTau *ex vivo*. Thus, we propose that PLA constitutes a favourable alternative to IHC when analysing co-pathology in different neurodegenerative disorders. Furthermore, considering its multiplexing potential, it could provide valuable insights into the role of potential cross-seeding mechanisms in the pathogenesis of different NDDs

## **Paper IV**

### **Temporal evolution of glial and peripheral inflammation prior to pSyn<sup>S129</sup> inclusion formation**

In paper IV, we performed intracerebral inoculations with ms PFFs in wt mice (n=30) to study early pathological and inflammatory events that take place from day 1 to 30 days post-injections (dpi) at regular time intervals. Our study aimed to elucidate the temporal relationship regarding inflammation and formation of pSynS129 inclusions. The paraffin-fixed brain sections were stained against pSyn<sup>S129</sup> species with in-house developed PLAs described in **paper II** and **III**. Furthermore, by using different glial and inflammatory markers we revealed temporal information regarding their cellular morphology changes that occur prior to inclusion formation. Furthermore, signs of peripheral inflammation were determined by analysing the levels of pro-inflammatory cytokines in the blood measured by MSD multiplex ELISA. Already after 1 dpi of PFFs, we observed a strong pSyn<sup>S129</sup> immunoreactivity close to the striatal

injection site. Intriguingly, this type of staining disappeared with the concurrent formation of peri-nuclear pSyn<sup>S129</sup> inclusions in motor and piriform cortex, amygdala and periventricular hypothalamus after 14 dpi. Concomitantly, we observed astrocytic activation as an early event happening prior to intracellular formation and propagation pSyn<sup>S129</sup> inclusions in the brain and peripheral organs. Our results indicate that a single PFF injection was enough to induce astrocytic activation (**Fig. 9**) and neuro-inflammatory response mediated by reactive astrocytes occurring prior to intra-neuronal accumulation and seeding of misfolded  $\alpha$ -syn. Although the cytokine profile between in whole did not significantly differ between PFF- and monomer-injected mice, changes in the levels of IL-6, KC/GRO and IL-10 could be observed at different time-points post injection within the PFF-injected mice.

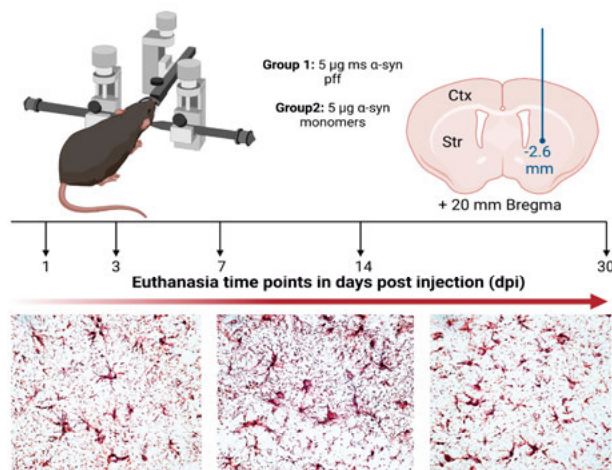


*Figure 9: Temporal evolution of astrocytic response.* After a single unilateral injection PFFs into the right dorsal striatum, ipsilateral GFAP+ astrocytes showed differences in their morphology at 1-, 14- and 30-days post-injection (dpi).

## Reflections and future perspectives

We developed several novel types of PLAs as an alternative approach for spatial visualization and detection of different  $\alpha$ -syn and tau aggregation species and / or their phosphorylated proteoforms *ex vivo*. We validated that this approach was both useful and successful to detect pathological species in AD and PD brains, in addition to animal models. We conclude that PLA is a technique with higher power in terms of *ex vivo* target specificity and sensitivity compared to regular IHC. However, with greater detection power comes greater scientific responsibility. Firstly, since PLA is a technique that relies on individual antibody epitope-selectivity, if used in an improper way the method might lead to a risk of amplifying cross-reactivity of antibodies several fold and thereby inducing false positive signal. Secondly, as PLA indicates *in situ* spatial proximity of two epitopes of respective proteins, it might not necessarily indicate a direct interaction between two proteins. Thirdly, PLA is a semi-quantitative technique and, if targets are present in abundance, it might lead to a ‘ceiling effect’ if the PLA protocol is not optimized in proper way.

While keeping above-mentioned risks in mind, our results have opened up several exciting opportunities to study fundamental scientific questions regarding the pathogenesis of AD and PD:

- 1) In what sub-cellular compartment does the S129 phosphorylation of  $\alpha$ -syn occur, and at which aggregation stage is  $\alpha$ -syn phosphorylated?
- 2) What molecular machinery do the apparent TNTs utilize in order to propagate pSyn<sup>S129</sup> species?
- 3) Can PLA against pSyn<sup>S129</sup> differentiate between inclusions observed in different anatomical locations in synucleinopathy patients, such as skin, duodenum, brainstem, cingulate cortex? Can it be employed as a peripheral biomarker in prodromal synucleinopathy patients?
- 4) Is tau hyper-phosphorylation a site-specific sequential phenomenon? What sites govern tau phosphorylation in PHF formation in the AD brain?
- 5) Can we analyse effects of different post-translational modification in the cross seeding of different pathological proteins?

# Populärvetenskaplig sammanfattning

Demens är ett mycket allvarligt problem för den person som drabbas, men även för anhöriga och samhället i stort. Det uppskattas av världshälsoorganisationen (WHO) att omkring 50 miljoner människor världen över för närvarande lider av någon typ av demenssjukdom. Det finns för närvarande ingen typ av botande behandling, utan idag kan bara symtomlindring erbjudas. Därför finns ett akut behov av att utarbeta nya strategier för ta fram behandlingar som kan stoppa själva sjukdomsprocessen.

De vanligaste demenssjukdomarna som orsakar nedbrytning av olika celltyper i specifika områden i hjärnan är Alzheimers sjukdom och Parkinsons sjukdom. Dessa sjukdomar drabbar främst äldre personer och antalet dödsfall de orsakar är det sjunde högsta räknat bland alla typer av sjukdomar. Om vi därför förbättrar möjligheten till en tidig diagnostik, och utvecklar mer effektiva behandlingsmetoder kommer det leda till en oerhörd nytta för drabbade patienter, anhöriga och samhället i stort.

Det finns flera likheter mellan Alzheimers sjukdom och Parkinsons sjukdom. Vid båda sjukdomarna kan felveckade proteiner ansamlas i olika typer av celler och på så vis bryta ner olika delar av hjärnan. Proteinansamlingarna vid Alzheimers sjukdom består huvudsakligen av proteinerna amyloid-beta och tau, medan vid Parkinsons sjukdom utgörs ansamlingarna av proteinet alfa-synuklein. Gemensamt för både tau och alfa-synuklein är att de av olika forskare beskrivs som "infektiösa proteiner". Orsaken till detta är att de felveckade formerna av tau och alfa-synuklein kan påverka de normala (friska) formerna av proteinerna att också felveckas och bilda skadliga ansamlingar. Både formförändringen och den resulterande ansamlingen av felveckade proteiner i hjärnan börjar ungefär 20 år innan symtomen uppstår.

För närvarande pågår forskning över hela världen för att förbättra teknikerna för hjärnabbildning (PET) och att mäta proteinförändringar i ryggmärgsvätska för att öka möjligheten till att ställa en tidigare och säkrare diagnos. Men mer forskning behövs för att förstå de underliggande sjukdomsmekanismerna för Alzheimers sjukdom och Parkinsons sjukdom. Den här avhandlingen har fokuserat på att identifiera de molekylära förändringarna i tau och alfa synuklein som sker vid demenssjukdomars. Tidigare studier har visat att felveckat tau

och alfa-synukleins förmåga att bilda skadliga ansamlingar kan påverkas genom att de kemiskt modifieras så att en fosfatgrupp binder till specifika delar av proteinerna. Syftet med det här arbetet har varit att i första hand undersöka förekomsten i hjärnan av ansamlingar av tau och alfa-synuklein som är modifierade med dessa fosfatgrupper. I vår forskargrupp har vi utvecklat en mycket känslig teknik som gör att vi snabbt och exakt kan mäta dessa molekylära förändringar som sker i hjärnan vid sjukdomarna.

Den fråga som jag tycker är mest intressant är hur länge vi kommer behöva vänta på att nya metoder för förbättrad diagnostik av sjukdomarna ska komma allmänheten till godo? Jag hoppas att vår forskning kommer att leda till utveckling av tester som kan bidra till att diagnostisera proteinförändringarna flera år i förväg och på så sett öppna möjligheterna till en tidigare behandling av våra vanligaste neurodegenerativa sjukdomar.

## सारांश | (sammanfattning på Marathi)

स्मृतीभ्रंश ही एक अतिशय गंभीर स्वरूपाची वैयक्तिक पण तरीही सामाजिक समस्या आहे. जगभरात सुमारे ५ कोटी लोक सध्या या व्याधीमुळे ग्रस्त असल्याचं अनुमान जागतिक आरोग्य संघटनेच्या (WHO) कडून वर्तविण्यात आलेलं आहे. त्यावर सद्यस्थितीला कोणताही उपचार उपलब्ध नाही. त्या अनुषंगाने येणाऱ्या अडचणीवर मात करण्यासाठी विविध प्रकारच्या योजना आखण्याची आत्यंतिक गरज आहे. ह्या स्मृतीभ्रंशाची अथवा मेंदूच्या उत्पीडन व न्हासाची प्रामुख्याने दोन कारणे दिली जातात. पहिले कारण म्हणजे अल्झायमरचा विकार आणि दुसरे कारण म्हणजे पार्किन्सनचा विकार. हे दोन्हीही विकार वयोवृद्ध लोकांमध्ये संभवतात. ह्या दोन विकारांमुळे होणारे मृत्यू जगभरात सर्वत्र होणाऱ्या मृत्यूंची तुलनेत सातव्या क्रमांकावर आहेत. त्यामुळे ह्या वयोवृद्ध लोकांमध्ये जर आपण त्वरित निदान व उपचार करण्याची पध्दती विकसित करून अमलात आणली तर कदाचित ह्या लोकांना, त्यांच्या नातेवाईकांना आणि समाजाला योग्य फायदा होईल.

ह्या दोन स्मृतीभ्रंशाच्या विकारांमध्ये साधर्म्य आढळते. पहिले साधर्म्य म्हणजे मेंदूच्या पेशींमध्ये तयार होणाऱ्या प्रथिनयुक्त गुठळ्या. दुसरे साधर्म्य म्हणजे मेंदू मधील ठराविक पेशींचा अथवा मज्जातंतूंचा ठराविक क्रमाने होणारा न्हास हे होय. अल्झायमर मध्ये आढळणाऱ्या प्रथिनयुक्त गुठळ्यांमध्ये प्रामुख्याने अमीलॉइड बीटा आणि टाऊ ह्या प्रथिन संचयांचा समावेश होतो. तर पार्किन्सन मध्ये अल्फा सिन्यूक्लीन हा प्रथिनसंचय आढळून येतो. टाऊ आणि अल्फा सिन्यूक्लीन ह्या दोन्ही प्रथिनांचा उल्लेख विविध वैज्ञानिक 'संक्रमक प्रथिने' असा करतात. यामागचे मुख्य कारण म्हणजे ही दोन्हीही प्रथिने त्यांच्या अनैसर्गिक स्थितीमध्ये इतर नैसर्गिक स्थितीमध्ये संभवणाऱ्या टाऊ आणि अल्फा सिन्यूक्लीन प्रथिनांमध्ये दोष निर्माण करून त्यांची गुठळी बनविण्यास प्रवृत्त करतात. ह्या दोन्हीही प्रथिनांमध्ये होणारा बदल आणि त्यामुळे मेंदूत होणारे प्रथिनांचे संचयन स्मृती-हास सुरु होण्यापूर्वी २० वर्षे आधी चालू झालेले असते पण दुर्दैवाने स्मृती न्हासाची लक्षणे अकस्मात दिसू लागतात.

सध्या ह्या दोन विकारांचे त्वरित निदान करण्याकरिता मेंदूचा PET scan अथवा मणक्यातील मज्जद्राव्य तपासणीच्या यंत्रणा विकसित करण्याचे संशोधन जगभर होत आहे. पण ह्या यंत्रणा जास्तीत जास्त रित्या अचूक करून १०० टक्के योग्य अंदाज वर्तविण्यासाठी अधिक संशोधन गरजेचे आहे. माझ्या संशोधनाचा विशेष भर टाऊ

आणि अल्फा सिन्यूक्लीन मध्ये होणाऱ्या रेण्विय बदलांवर आधारित आहे. ह्या दोन प्रथिनांमध्ये होणारे बिघाड आणि त्यामुळं होणारे त्यांचे संचयन ह्याचा जवळचा संबंध त्यांच्यामध्ये होणाऱ्या विविध प्रकारच्या फॉस्फरस रेणुंच्या संरचनेवर आधारित असल्याचे निरीक्षण नोंदवले गेले आहे. माझे काम हे प्रामुख्याने क्रमशः रित्या होणाऱ्या ह्या रेण्विय बदलांचा तपास करणे हे आहे. माझ्या संशोधनामध्ये मी एक अतिशय संवेदनशील अशी तंत्रप्रणाली विकसित केली आहे, ज्यायोगे आपल्याला विकारयुक्त मेंदू मध्ये होणाऱ्या रेण्विय बदलांचे प्रमाण लवकरच व अचूकपणे दिसून येते.

आता चित्तवेधक मुद्दा असा की येत्या काही वर्षात, माझे संशोधन आणि इतर प्रयोगशाळा आणि रुग्णालयांमध्ये होणारे संशोधन ह्यांची सांगड घालून एखादी अशी तपासणी यंत्रणा विकसित होऊन सर्वसामान्यांपर्यंत पोहोचण्यासाठी आपल्याला किती वाट बघावी लागेल ? पण मी अशी आशा करतो की माझ्या संशोधनाच्या आधारे अशी एखादी चाचणी विकसित होईल की ज्या योगे ह्या गंभीर प्रथिन बदलांचे निदान अचूकपणे कित्येक वर्षे आधीच स्पष्ट होऊ शकेल आणि त्यायोगे वैद्यकीय कर्मचाऱ्यांना प्रतिबंधात्मक उपाययोजना करणे शक्य होईल. असे झाल्यास स्मृतीभ्रंश ग्रस्त व्यक्तीस, त्याच्या कुटुंबास आणि समाजास तो मोठा दिलासा ठरेल.

# Acknowledgements

This work was supported financially by Grants from Swedish Research Council (MI:2018-03075, 2021-02793), Torsten Söderberg Foundation, Swedish Parkinson Foundation, Swedish Brain Foundation, Swedish Alzheimer Foundation, Swedish Dementia Association, Magnus Bergwall Foundation, Åhlén Foundation, King Gustaf V's, and Queen Victoria's Freemason Foundation, Sigurd and Elsa Golje's Foundation, Stohne's Foundation, Gamla Tjänarinnor Foundation.

The last four and half years have come to a pass and now it is time to bid adieu to everyone who is part of my academic journey leading towards a PhD. During the past four years, I was very lucky to have four PhD advisors or rather, my 'four pillars'. Relying on these four pillars, I could build my PhD studies, with each of them having a unique quality that I tried to learn and cultivate over the last few years. Time will only tell if I will be able to do them justice.

**'Pragmatism'** is the quality that I tried to learn from you **Sara!** When I came to this lab, I was a young and naïve masters' student; you took me under your wing and mentored me in the world of 'animal behaviour and neuroscience'. You are a very organized and skilful person especially with your awe-inspiring rapid surgical skills. I learnt all the practical skills that one needs for navigating in the lab, while working with animals and for all the day-to-day planning work! I wish I had more time with you to continue our experiments further, as you always brought positive energy with your friendly smile.

**'Proficiency'** is the quality that I admire the most in you, **Stina!** Your brilliance with your scientific presentations, soft-skills and network-building skills is unmatched. You are a fantastic boss!

**'Prudence'** is my word for you **Martin!** Apart from your phenomenal capacity to multi-task and manage people, plan and execute complex scientific projects, you also have a futuristic perspective and scientific vision. That is a rare quality and I feel lucky to have been able to learn from you. I always enjoyed engaging in scientific discussions with you while also seeking advice from you. I hope you are getting plenty of opportunity for skiing in Canada as a winter person! 😊

**Joakim**, although you are my main advisor, yet I made you wait until this page. But as they say ‘all the good things in due time’. You are a personification of the word ‘**panache**’! I learnt one of the most important things in my life from you- no matter how skilled and successful you are as a researcher; a true scientist is always driven by a passion and curiosity for life itself. You taught me that this curiosity has no limits- let it be about ATTR or Cheetah Amyloid, Alpha-synuclein, HNE/ONE-oligomers, synaptic proteins or BASEBALL, SHOES, and WINE for that matter. You also taught me to ‘kill my darlings’ when it comes to writing a manuscript, and made me a more grounded and realistic researcher. I am grateful for your thoughtfulness and generosity with your time, even when little Astrid needed you more than I did! I will be truly grateful for everything you have done for me, and will miss your insights into life and your very discerning sense of humour!

I would like to express my gratitude to all the collaborators, co-authors and all the people with whom I was involved with other scientific projects from Uppsala University and Uppsala Academic Hospital. Thank you for all your help with HPLC: **Per-Ove Thörnqvist**, **Svante Winberg** from the former Neuroscience department. **Dag Nyholm**, **Paul de Roos** and **Per Hellström** from the Uppsala Academic Hospital, for showing me the clinical side of Parkinson’s disease. **Monika Hodik** thanks for your help with the electron microscope. **Dominic Luc-Webb** for all your help with multiplex ELISA plate reader. I would also like to thank all my past students: **Sheyma**, **Nancy**, **Moa** and **Emma H.** for putting in all the wonderful experimental work and adding so much to the scientific discussions we had. I wish you all the very best for your current and future endeavours! 😊

All the UU innovation people, **Hillevi** and **Kerstin** thank you for the opportunities you gave me and for helping me see the commercial potential of one’s scientific ideas. **Cecilia**, you are an amazing mentor and you always had time for me from your busy schedule, I appreciate your guidance, helping me build a perspective about subtle differences in academic and corporate worlds of scientific research.

**Anna**, you were always a great company for Fika breaks and having nice discussions. Thank you for your insightful feedback on my manuscript, I appreciate it a lot. **Dag Sehlin**, (mentioning your last name, because there is another ‘Dag’ in acknowledgements), I always admired you for being the ‘ELISA king’, your scientific integrity, and your amazing talent in baking croissants! I enjoyed our ‘Padel tennis’ session together with Joakim and Maria, maybe we should do it more often. **Vilmantas**, you were always a great help with computer and electronics, I wish I were as tech savvy as you. **Ximena**, thank you for all your help in the lab, your amazing tiramisù, and for getting exotic

flavours of KitKat for me all the way from Japan. **Greta**, I will always admire you for your innovative scientific approach and Beach Volley skills.

To all the MolGers that started or finished their PhD journey before me- **Leire**, **Tsong**, **Elisabeth**, **Jinar**, **Silvio**, **Maria**, **Tobbe G**, **Emma B** and **Evangelos** you people were the ‘OGs’ and without your support in the lab and your friendship, it would have been difficult to survive the ‘PhD blues’. With each one of you, I share a personal bond and I will cherish all our memories in my heart forever. **Leire** and **Tsong**, thank you for your beautiful wedding, which gave me wonderful new memories with all our colleagues. **Jinar**, you are a warm and generous friend that I will treasure always, along with your hand-knitted mössa that keeps my ears cosy. **Silvio**, I miss your Apfel Strudel and Raclette nights. I forgive you for calling me a ‘source of gossip’ in your acknowledgements ;-)  
**Tobbe G**, aka **Big T**, I could not have asked for a better desk partner. Your Nordic-noir humour made my long days at the lab fun! I wish you all the success- you have the soul of a true academic. May you never fall short of weird YouTube videos. **Emma B**, thank you for your cheerful presence and optimism. You brighten all our lives! **Evangelos** you will already be done with your PhD when you read this- hearty congratulations!

To all the current PhD students from MolGer, you are the future PhDs and I am sure you will do an amazing job. **Rebecca**, you are a cool and creative person, and I always had a great time at your Norwegian pancake / board game evenings. **Mengfei**, you are full of quiet fun and a pleasure to talk to. Good luck with your PET adventures! **Eva**, aka ‘**Frau Schlein**’ thank you for all the delicious dishes you prepared, and all the discussions and engaging conversations we had. I wish you luck with everything and hopefully one day, you will be able to do ‘one-arm pull-up’ as well! **Gillian** thanks for bringing us your Canadian sweetness along with the maple syrup. **Tobias M.** aka **lil’ Tobbe** hopefully one day you will succeed in opening a luxury Swedish sauna hotel that will serve your handcrafted, finely micro-brewed ‘Tau beers’.

To the newly joined members of MolGer: **Sara Lopes**, **Wojciech**, **Abdul** and **Amelia**, welcome to the best group! Thank you for all the nice coffee and conversations we had in this short time together. I would also like to express my deepest gratitude to all the current and former members of MolGer: **Astrid**, **Agata**, **Agnieszka**, **Ropafadzo**, **Chiara**, **Gabriel**, **Veronica**, **Elisabeth I.**, **Elina**, **Johanna**, **Sahar**, **Ulrika**, **Linn**, **Marlena**, **Gustaf**, **Bodil**, **Lars**, and **Elin**.

All the Rudbeck corridor people: **Maryam**, **Moeen**, **Mehran**, **Anna**, **Anzhelika** thank you for all the ‘after-works’ and helping me blow some steam off after hectic and long working days!

**Nadja** and **Alice**, the young scientists next door, thank you for all the neighbourly Fika times and conversations at work and outside work.

My water polo teammates from USS Vattenpolo: **Axel, Fredrik, Shaun, Johan, João, Jeroen, Laura** and all the others for keeping my ‘fighting spirit’ ‘alive’ and ‘kicking’. A PhD can be an isolating journey and I would have had a much tougher time if not for our team. ☺

My beach volley and physicist friends: **Inga, Merle, Anna, Eike, Björn, Georgii** and **Antonino**. Thank you for all the games we have had together, it is always fun to de-stress and enjoy the (rare) sunny summer day in Uppsala after spending endless days indoors at a lab.

To my beautiful Uppsala family: **Fadi, Mikaela, Philipp, Melanie**, and **David** you are my backbone. Words would not do proper justice for your unconditional support through happy and tough times. You are what makes Uppsala home. Thank you from the bottom of my heart!

My lifelines, originally from the P-town, **Pune**, but now scattered all over the world: **Suvrat** aka ‘**Sugya**’ **Apte**, **Advait** aka ‘**Adya**’ **Deshmukh**, **Amish** aka ‘**Baadshah**’ **Sarpotdar**, **Tanveer** aka ‘**Manu**’ **Teranikar**, **Varun** aka ‘**The Doctor**’ **Solanki** and the last but not least **Nakul** aka ‘**Baku**’ **Raval**. Straight outta murky alleys of Vaishali, Cosmos, and Sarang to here-, we have all come a long way from home. Looking forward to more adventures in the lavish squares in New York, Boston, Houston, Philly, and Manchester!

To my family, **Aai, Baba, Lilu** and my grandmothers **Sunanda Ajji** and **Nalini Ajji**, thank you for helping and supporting me with your life! My late grandfathers, **Anna** and **Abaa**, your presence is still bright in my memory.

Lastly, to **Rashmi**, who would probably want to edit these acknowledgements- thank you for always believing in me and having my back. I am lucky to have you around, even though you sometimes refuse to move from the sofa and make my Netflix recommendations full of K-dramas.

## References:

1. Smith, L. M. & Kelleher, N. L. Proteoform: a single term describing protein complexity. *Nat. Methods* **10**, 186–187 (2013).
2. The Human Proteoform Project: Defining the human proteome. <https://www.science.org/doi/10.1126/sciadv.abk0734> doi:10.1126/sciadv.abk0734.
3. Aebersold, R. *et al.* How many human proteoforms are there? *Nat. Chem. Biol.* **14**, 206–214 (2018).
4. Anfinsen, C. B. Principles that govern the folding of protein chains. *Science* **181**, 223–230 (1973).
5. Levinthal, C. Are there pathways for protein folding? *J. Chim. Phys.* **65**, 44–45 (1968).
6. Dill, K. A. & Chan, H. S. From Levinthal to pathways to funnels. *Nat. Struct. Mol. Biol.* **4**, 10–19 (1997).
7. Durup, J. On “Levinthal paradox” and the theory of protein folding. *J. Mol. Struct. THEOCHEM* **424**, 157–169 (1998).
8. Dinner, A. R., Šali, A., Smith, L. J., Dobson, C. M. & Karplus, M. Understanding protein folding via free-energy surfaces from theory and experiment. *Trends Biochem. Sci.* **25**, 331–339 (2000).
9. Mayor, U. *et al.* The complete folding pathway of a protein from nanoseconds to microseconds. *Nature* **421**, 863–867 (2003).
10. Fulton, A. B. How crowded is the cytoplasm? *Cell* **30**, 345–347 (1982).
11. Guigas, G., Kalla, C. & Weiss, M. Probing the Nanoscale Viscoelasticity of Intracellular Fluids in Living Cells. *Biophys. J.* **93**, 316–323 (2007).
12. Hartl, F. U. Molecular chaperones in cellular protein folding. **381**, 10 (1996).
13. Ellis, R. J. Molecular chaperones: assisting assembly in addition to folding. *Trends Biochem. Sci.* **31**, 395–401 (2006).
14. Posttranslational Quality Control: Folding, Refolding, and Degrading Proteins | Science. <https://www.science.org/doi/full/10.1126/science.286.5446.1888>.
15. Dobson, C. M. Protein folding and misfolding. **426**, 7 (2003).
16. Chiti, F. & Dobson, C. M. Protein Misfolding, Functional Amyloid, and Human Disease. *Annu. Rev. Biochem.* **75**, 333–366 (2006).
17. Li, S.-H. & Li, X.-J. Aggregation of N-Terminal Huntingtin is Dependent on the Length of Its Glutamine Repeats. *Hum. Mol. Genet.* **7**, 777–782 (1998).
18. Novel Proteinaceous Infectious Particles Cause Scrapie. <https://www.science.org/doi/10.1126/science.6801762> doi:10.1126/science.6801762.
19. Lachmann, H. J. *et al.* Natural History and Outcome in Systemic AA Amyloidosis. *N. Engl. J. Med.* **356**, 2361–2371 (2007).
20. J, G. *et al.* Genetic Alterations of the BRI2 gene: Familial British and Danish Dementias. *Brain Pathol.* **16**, 71–79 (2006).
21. Hardy, J. A. & Higgins, G. A. Alzheimer’s Disease: The Amyloid Cascade Hypothesis. *Science* **256**, 184–185 (1992).

22. Hardy, J. & Selkoe, D. J. The Amyloid Hypothesis of Alzheimer's Disease: Progress and Problems on the Road to Therapeutics. *Science* **297**, 353–356 (2002).
23. Polvikoski, T. *et al.* Apolipoprotein E, Dementia, and Cortical Deposition of  $\beta$ -Amyloid Protein. *N. Engl. J. Med.* **333**, 1242–1248 (1995).
24. Zhang, Y., Wu, K.-M., Yang, L., Dong, Q. & Yu, J.-T. Tauopathies: new perspectives and challenges. *Mol. Neurodegener.* **17**, 28 (2022).
25. Braak, H. & Braak, E. Neuropathological staging of Alzheimer-related changes. *Acta Neuropathol. (Berl.)* **82**, 239–259 (1991).
26. Koller, E. J. *et al.* Combining P301L and S320F tau variants produces a novel accelerated model of tauopathy. *Hum. Mol. Genet.* **28**, 3255–3269 (2019).
27. Goedert, M., Jakes, R. & Spillantini, M. G. The Synucleinopathies: Twenty Years On. *J. Park. Dis.* **7**, S51–S69.
28. McCann, H., Stevens, C. H., Cartwright, H. & Halliday, G. M.  $\alpha$ -Synucleinopathy phenotypes. *Parkinsonism Relat. Disord.* **20**, S62–S67 (2014).
29. Spillantini, M. G. *et al.*  $\alpha$ -Synuclein in Lewy bodies. *Nature* **388**, 839–840 (1997).
30. Aarsland, D. *et al.* Frequency and case identification of dementia with Lewy bodies using the revised consensus criteria. *Dement. Geriatr. Cogn. Disord.* **26**, 445–452 (2008).
31. Jellinger, K. A. & Korczyn, A. D. Are dementia with Lewy bodies and Parkinson's disease dementia the same disease? *BMC Med.* **16**, (2018).
32. Arnaoutoglou, N. A., O'Brien, J. T. & Underwood, B. R. Dementia with Lewy bodies — from scientific knowledge to clinical insights. *Nat. Rev. Neurol.* **15**, 103–112 (2019).
33. Grazia Spillantini, M. *et al.* Filamentous  $\alpha$ -synuclein inclusions link multiple system atrophy with Parkinson's disease and dementia with Lewy bodies. *Neurosci. Lett.* **251**, 205–208 (1998).
34. Wakabayashi, K., Yoshimoto, M., Tsuji, S. & Takahashi, H.  $\alpha$ -Synuclein immunoreactivity in glial cytoplasmic inclusions in multiple system atrophy. *Neurosci. Lett.* **249**, 180–182 (1998).
35. Fanciulli, A. & Wenning, G. K. Multiple-System Atrophy. *N. Engl. J. Med.* **372**, 249–263 (2015).
36. Dementia. <https://www.who.int/news-room/fact-sheets/detail/dementia>.
37. Maurer, K., Volk, S. & Gerbaldo, H. Auguste D and Alzheimer's disease. *The Lancet* **349**, 1546–1549 (1997).
38. Stelzmann, R. A., Norman Schnitzlein, H. & Reed Murtagh, F. An english translation of alzheimer's 1907 paper, 'über eine eigenartige erkankung der hirnrinde?' *Clin. Anat.* **8**, 429–431 (1995).
39. Hyman, B. T. *et al.* National Institute on Aging–Alzheimer's Association guidelines for the neuropathologic assessment of Alzheimer's disease. *Alzheimers Dement. J. Alzheimers Assoc.* **8**, 1–13 (2012).
40. NIA-AA Research Framework: Toward a biological definition of Alzheimer's disease. *Alzheimers Dement.* **14**, 535–562 (2018).
41. Hansson, O. Biomarkers for neurodegenerative diseases. *Nat. Med.* **27**, 954–963 (2021).
42. Thijssen, E. H. *et al.* Association of Plasma P-tau217 and P-tau181 with clinical phenotype, neuropathology, and imaging markers in Alzheimer's disease and frontotemporal lobar degeneration: a retrospective diagnostic performance study. *Lancet Neurol.* **20**, 739–752 (2021).

43. Palmqvist, S. *et al.* Discriminative Accuracy of Plasma Phospho-tau217 for Alzheimer Disease vs Other Neurodegenerative Disorders. *JAMA* **324**, 772–781 (2020).
44. Kumar, K., Kumar, A., Keegan, R. M. & Deshmukh, R. Recent advances in the neurobiology and neuropharmacology of Alzheimer’s disease. *Biomed. Pharmacother. Biomedecine Pharmacother.* **98**, 297–307 (2018).
45. Research, C. for D. E. and. Aducanumab (marketed as Aduhelm) Information. *FDA* (2021).
46. Tanner, C. M. & Goldman, S. M. EPIDEMIOLOGY OF PARKINSON’S DISEASE. *Neurol. Clin.* **14**, 317–335 (1996).
47. Kalia, L. V. & Lang, A. E. Parkinson’s disease. *Lancet Lond. Engl.* **386**, 896–912 (2015).
48. Del Tredici, K. & Braak, H. Dysfunction of the locus coeruleus-norepinephrine system and related circuitry in Parkinson’s disease-related dementia. *J. Neurol. Neurosurg. Psychiatry* **84**, 774–783 (2013).
49. Halliday, G. M., Blumbergs, P. C., Cotton, R. G., Blessing, W. W. & Geffen, L. B. Loss of brainstem serotonin- and substance P-containing neurons in Parkinson’s disease. *Brain Res.* **510**, 104–107 (1990).
50. Hirsch, E. C., Graybiel, A. M., Duyckaerts, C. & Javoy-Agid, F. Neuronal loss in the pedunculopontine tegmental nucleus in Parkinson disease and in progressive supranuclear palsy. *Proc. Natl. Acad. Sci. U. S. A.* **84**, 5976–5980 (1987).
51. Jellinger, K. The pedunculopontine nucleus in Parkinson’s disease, progressive supranuclear palsy and Alzheimer’s disease. *J. Neurol. Neurosurg. Psychiatry* **51**, 540–543 (1988).
52. Braak, H. *et al.* Staging of brain pathology related to sporadic Parkinson’s disease. *Neurobiol. Aging* **24**, 197–211 (2003).
53. Schapira, A. H. V., Chaudhuri, K. R. & Jenner, P. Non-motor features of Parkinson disease. *Nat. Rev. Neurosci.* **18**, 435–450 (2017).
54. Grinberg, L. T., Rueb, U., Alho, A. T. di L. & Heinsen, H. Brainstem pathology and non-motor symptoms in PD. *J. Neurol. Sci.* **289**, 81–88 (2010).
55. Shah Nawaz, M. *et al.* Discriminating  $\alpha$ -synuclein strains in Parkinson’s disease and multiple system atrophy. *Nature* **578**, 273–277 (2020).
56. Donadio, V. *et al.* Skin  $\alpha$ -synuclein deposits differ in clinical variants of synucleinopathy: an in vivo study. *Sci. Rep.* **8**, (2018).
57. Bonifati, V. *et al.* Mutations in the DJ-1 gene associated with autosomal recessive early-onset parkinsonism. *Science* **299**, 256–259 (2003).
58. Kitada, T. *et al.* Mutations in the parkin gene cause autosomal recessive juvenile parkinsonism. *Nature* **392**, 605–608 (1998).
59. Polymeropoulos, M. H. *et al.* Mutation in the alpha-synuclein gene identified in families with Parkinson’s disease. *Science* **276**, 2045–2047 (1997).
60. Valente, E. M. *et al.* Hereditary early-onset Parkinson’s disease caused by mutations in PINK1. *Science* **304**, 1158–1160 (2004).
61. Zimprich, A. *et al.* Mutations in LRRK2 cause autosomal-dominant parkinsonism with pleomorphic pathology. *Neuron* **44**, 601–607 (2004).
62. Moore, D. J., West, A. B., Dawson, V. L. & Dawson, T. M. Molecular Pathophysiology of Parkinson’s Disease. *Annu. Rev. Neurosci.* **28**, 57–87 (2005).
63. Bronstein, J. M. *et al.* Deep Brain Stimulation for Parkinson Disease. *Arch. Neurol.* **68**, 165–171 (2011).

64. Connolly, B. S. & Lang, A. E. Pharmacological treatment of Parkinson disease: a review. *JAMA* **311**, 1670–1683 (2014).
65. Weingarten, M. D., Lockwood, A. H., Hwo, S. Y. & Kirschner, M. W. A protein factor essential for microtubule assembly. *Proc. Natl. Acad. Sci. U. S. A.* **72**, 1858–1862 (1975).
66. Cleveland, D. W., Hwo, S.-Y. & Kirschner, M. W. Physical and chemical properties of purified tau factor and the role of tau in microtubule assembly. *J. Mol. Biol.* **116**, 227–247 (1977).
67. Grundke-Iqbal, I. *et al.* Abnormal phosphorylation of the microtubule-associated protein tau ( $\tau$ ) in Alzheimer cytoskeletal pathology. *Proc. Natl. Acad. Sci. U. S. A.* **83**, 4913–4917 (1986).
68. Goedert, M., Spillantini, M. G., Potier, M. C., Ulrich, J. & Crowther, R. A. Cloning and sequencing of the cDNA encoding an isoform of microtubule-associated protein tau containing four tandem repeats: differential expression of tau protein mRNAs in human brain. *EMBO J.* **8**, 393–399 (1989).
69. Hirokawa, N., Shiomura, Y. & Okabe, S. Tau proteins: the molecular structure and mode of binding on microtubules. *J. Cell Biol.* **107**, 1449–1459 (1988).
70. Steiner, B. *et al.* Phosphorylation of microtubule-associated protein tau: identification of the site for Ca<sup>2+</sup>(+)-calmodulin dependent kinase and relationship with tau phosphorylation in Alzheimer tangles. *EMBO J.* **9**, 3539–3544 (1990).
71. Mukrasch, M. D. *et al.* Structural polymorphism of 441-residue tau at single residue resolution. *PLoS Biol.* **7**, e34 (2009).
72. Kosik, K. S., Orecchio, L. D., Bakalis, S. & Neve, R. L. Developmentally regulated expression of specific tau sequences. *Neuron* **2**, 1389–1397 (1989).
73. Sultan, A. *et al.* Nuclear tau, a key player in neuronal DNA protection. *J. Biol. Chem.* **286**, 4566–4575 (2011).
74. Papasozomenos, S. C. & Binder, L. I. Phosphorylation determines two distinct species of Tau in the central nervous system. *Cell Motil. Cytoskeleton* **8**, 210–226 (1987).
75. Goldbaum, O. *et al.* Proteasome inhibition stabilizes tau inclusions in oligodendroglial cells that occur after treatment with okadaic acid. *J. Neurosci. Off. J. Soc. Neurosci.* **23**, 8872–8880 (2003).
76. Askanas, V., Engel, W. K., Alvarez, R. B., McFerrin, J. & Broccolini, A. Novel Immunolocalization of  $\alpha$ -Synuclein in Human Muscle of Inclusion-Body Myositis, Regenerating and Necrotic Muscle Fibers, and at Neuromuscular Junctions. *J. Neuropathol. Exp. Neurol.* **59**, 592–598 (2000).
77. Braak, E., Braak, H. & Mandelkow, E.-M. A sequence of cytoskeleton changes related to the formation of neurofibrillary tangles and neuropil threads. 14.
78. Dixit, R., Ross, J. L., Goldman, Y. E. & Holzbaur, E. L. F. Differential regulation of dynein and kinesin motor proteins by tau. *Science* **319**, 1086–1089 (2008).
79. Kimura, T. *et al.* Microtubule-associated protein tau is essential for long-term depression in the hippocampus. *Philos. Trans. R. Soc. Lond. B. Biol. Sci.* **369**, 20130144 (2014).
80. Köpke, E. *et al.* Microtubule-associated protein tau. Abnormal phosphorylation of a non-paired helical filament pool in Alzheimer disease. *J. Biol. Chem.* **268**, 24374–24384 (1993).
81. Fitzpatrick, A. W. P. *et al.* Cryo-EM structures of tau filaments from Alzheimer’s disease. *Nature* **547**, 185–190 (2017).

82. Lau, L., Schachter, J. B., Seymour, P. A. & Sanner, M. A. Tau Protein Phosphorylation as a Therapeutic Target in Alzheimers Disease. *Curr. Top. Med. Chem.* **2**, 395–415.
83. Goedert, M. *et al.* Assembly of microtubule-associated protein tau into Alzheimer-like filaments induced by sulphated glycosaminoglycans. *Nature* **383**, 550–553 (1996).
84. Alonso, A., Zaidi, T., Novak, M., Grundke-Iqbal, I. & Iqbal, K. Hyperphosphorylation induces self-assembly of tau into tangles of paired helical filaments/straight filaments. *Proc. Natl. Acad. Sci. U. S. A.* **98**, 6923–6928 (2001).
85. Biernat, J., Gustke, N., Drewes, G., Mandelkow, E. M. & Mandelkow, E. Phosphorylation of Ser262 strongly reduces binding of tau to microtubules: distinction between PHF-like immunoreactivity and microtubule binding. *Neuron* **11**, 153–163 (1993).
86. Schneider, A., Biernat, J., von Bergen, M., Mandelkow, E. & Mandelkow, E.-M. Phosphorylation that Detaches Tau Protein from Microtubules (Ser262, Ser214) Also Protects It against Aggregation into Alzheimer Paired Helical Filaments. *Biochemistry* **38**, 3549–3558 (1999).
87. Lin, Y.-T. *et al.* The binding and phosphorylation of Thr231 is critical for Tau's hyperphosphorylation and functional regulation by glycogen synthase kinase 3 $\beta$ . *J. Neurochem.* **103**, 802–813 (2007).
88. Jeganathan, S. *et al.* Proline-directed Pseudo-phosphorylation at AT8 and PHF1 Epitopes Induces a Compaction of the Paperclip Folding of Tau and Generates a Pathological (MC-1) Conformation \*. *J. Biol. Chem.* **283**, 32066–32076 (2008).
89. Morishima-Kawashima, M. *et al.* Proline-directed and Non-proline-directed Phosphorylation of PHF-tau (\*). *J. Biol. Chem.* **270**, 823–829 (1995).
90. Yu, Y. *et al.* Developmental regulation of tau phosphorylation, tau kinases, and tau phosphatases. *J. Neurochem.* **108**, 1480–1494 (2009).
91. Hanger, D. P., Betts, J. C., Loviny, T. L. F., Blackstock, W. P. & Anderton, B. H. New Phosphorylation Sites Identified in Hyperphosphorylated Tau (Paired Helical Filament-Tau) from Alzheimer's Disease Brain Using Nano-electrospray Mass Spectrometry. *J. Neurochem.* **71**, 2465–2476 (1998).
92. Greenberg, S. G. & Davies, P. A preparation of Alzheimer paired helical filaments that displays distinct tau proteins by polyacrylamide gel electrophoresis. *Proc. Natl. Acad. Sci. U. S. A.* **87**, 5827–5831 (1990).
93. Goedert, M. *et al.* Epitope mapping of monoclonal antibodies to the paired helical filaments of Alzheimer's disease: identification of phosphorylation sites in tau protein. *Biochem. J.* **301** ( Pt 3), 871–877 (1994).
94. Seubert, P. *et al.* Detection of phosphorylated Ser262 in fetal tau, adult tau, and paired helical filament tau. *J. Biol. Chem.* **270**, 18917–18922 (1995).
95. Kac, P. R. *et al.* Diagnostic value of serum versus plasma phospho-tau for Alzheimer's disease. *Alzheimers Res. Ther.* **14**, 65 (2022).
96. Stefanoska, K. *et al.* Alzheimer's disease: Ablating single master site abolishes tau hyperphosphorylation. *Sci. Adv.* **8**, eabl8809 (2022).
97. Clavaguera, F. *et al.* 'Prion-like' templated misfolding in tauopathies. *Brain Pathol. Zurich Switz.* **23**, 342–349 (2013).
98. Serrano-Pozo, A., Frosch, M. P., Masliah, E. & Hyman, B. T. Neuropathological Alterations in Alzheimer Disease. *Cold Spring Harb. Perspect. Med.* **1**, a006189 (2011).

99. Takeda, S. Tau Propagation as a Diagnostic and Therapeutic Target for Dementia: Potentials and Unanswered Questions. *Front. Neurosci.* **13**, 1274 (2019).
100. Wang, Y. & Mandelkow, E. Tau in physiology and pathology. *Nat. Rev. Neurosci.* **17**, 22–35 (2016).
101. Dujardin, S. *et al.* Tau molecular diversity contributes to clinical heterogeneity in Alzheimer’s disease. *Nat. Med.* **26**, 1256–1263 (2020).
102. Calafate, S. *et al.* Synaptic Contacts Enhance Cell-to-Cell Tau Pathology Propagation. *Cell Rep.* **11**, 1176–1183 (2015).
103. Pooler, A. M., Phillips, E. C., Lau, D. H. W., Noble, W. & Hanger, D. P. Physiological release of endogenous tau is stimulated by neuronal activity. *EMBO Rep.* **14**, 389–394 (2013).
104. Wu, J. W. *et al.* Neuronal activity enhances tau propagation and tau pathology in vivo. *Nat. Neurosci.* **19**, 1085–1092 (2016).
105. Falcon, B., Noad, J., McMahon, H., Randow, F. & Goedert, M. Galectin-8-mediated selective autophagy protects against seeded tau aggregation. *J. Biol. Chem.* **293**, 2438–2451 (2018).
106. Takeda, S. *et al.* Neuronal uptake and propagation of a rare phosphorylated high-molecular-weight tau derived from Alzheimer’s disease brain. *Nat. Commun.* **6**, 8490 (2015).
107. Wang, Y. *et al.* The release and trans-synaptic transmission of Tau via exosomes. *Mol. Neurodegener.* **12**, 5 (2017).
108. Chung, D. C., Roemer, S., Petrucelli, L. & Dickson, D. W. Cellular and pathological heterogeneity of primary tauopathies. *Mol. Neurodegener.* **16**, 57 (2021).
109. Maroteaux, L., Campanelli, J. & Scheller, R. Synuclein: a neuron-specific protein localized to the nucleus and presynaptic nerve terminal. *J. Neurosci.* **8**, 2804–2815 (1988).
110. George, J. M. The synucleins. *Genome Biol.* **3**, reviews3002.1 (2001).
111. Iwai, A. *et al.* The precursor protein of non-A $\beta$  component of Alzheimer’s disease amyloid is a presynaptic protein of the central nervous system. *Neuron* **14**, 467–475 (1995).
112. Jakes, R., Spillantini, M. G. & Goedert, M. Identification of two distinct synucleins from human brain. *FEBS Lett.* **345**, 27–32 (1994).
113. Baltic, S. *et al.*  $\alpha$ -Synuclein Is Expressed in Different Tissues During Human Fetal Development. *J. Mol. Neurosci.* **22**, 199–204 (2004).
114. Nakai, M. *et al.* Expression of  $\alpha$ -synuclein, a presynaptic protein implicated in Parkinson’s disease, in erythropoietic lineage. *Biochem. Biophys. Res. Commun.* **358**, 104–110 (2007).
115. Tamo, W. *et al.* Expression of  $\alpha$ -synuclein, the precursor of non-amyloid b component of Alzheimer’s disease amyloid, in human cerebral blood vessels. *Neurosci. Lett.* **4** (2002).
116. Chandra, S., Chen, X., Rizo, J., Jahn, R. & Südhof, T. C. A Broken  $\alpha$ -Helix in Folded  $\alpha$ -Synuclein. *J. Biol. Chem.* **278**, 15313–15318 (2003).
117. Sode, K., Ochiai, S., Kobayashi, N. & Usuzaka, E. Effect of Reparation of Repeat Sequences in the Human  $\alpha$ -Synuclein on Fibrillation Ability. *Int. J. Biol. Sci.* **3**, 1–7 (2006).
118. Krüger, R. *et al.* AlaSOPro mutation in the gene encoding  $\alpha$ -synuclein in Parkinson’s disease. *Nat. Genet.* **18**, 106–108 (1998).
119. Zarranz, J. J. *et al.* The new mutation, E46K, of  $\alpha$ -synuclein causes parkinson and Lewy body dementia. *Ann. Neurol.* **55**, 164–173 (2004).

120. Appel-Cresswell, S. *et al.* Alpha-synuclein p.H50Q, a novel pathogenic mutation for Parkinson's disease. *Mov. Disord.* **28**, 811–813 (2013).
121. Lesage, S. *et al.* G51D  $\alpha$ -synuclein mutation causes a novel Parkinsonian–pyramidal syndrome. *Ann. Neurol.* **73**, 459–471 (2013).
122. Pasanen, P. *et al.* A novel  $\alpha$ -synuclein mutation A53E associated with atypical multiple system atrophy and Parkinson's disease-type pathology. *Neurobiol. Aging* **35**, 2180.e1–2180.e5 (2014).
123. Yoshino, H. *et al.* Homozygous alpha-synuclein p.A53V in familial Parkinson's disease. *Neurobiol. Aging* **57**, 248.e7–248.e12 (2017).
124. Ibáñez, P. *et al.* Causal relation between  $\alpha$ -synuclein locus duplication as a cause of familial Parkinson's disease. *The Lancet* **364**, 1169–1171 (2004).
125. Singleton, A. B. *et al.*  $\alpha$ -Synuclein Locus Triplication Causes Parkinson's Disease. *Science* **302**, 841–841 (2003).
126. Kapasi, A. *et al.* A novel SNCA E83Q mutation in a case of dementia with Lewy bodies and atypical frontotemporal lobar degeneration. *Neuropathol. Off. J. Jpn. Soc. Neuropathol.* **40**, 620–626 (2020).
127. Ulmer, T. S., Bax, A., Cole, N. B. & Nussbaum, R. L. Structure and dynamics of micelle-bound human alpha-synuclein. *J. Biol. Chem.* **280**, 9595–9603 (2005).
128. Burré, J. The Synaptic Function of  $\alpha$ -Synuclein. *J. Park. Dis.* **5**, 699–713.
129. Burré, J. *et al.*  $\alpha$ -Synuclein Promotes SNARE-Complex Assembly in vivo and in vitro. *Science* **329**, 1663–1667 (2010).
130. Scott, D. & Roy, S.  $\alpha$ -Synuclein Inhibits Intersynaptic Vesicle Mobility and Maintains Recycling-Pool Homeostasis. *J. Neurosci.* **32**, 10129–10135 (2012).
131. Scott, D. A. *et al.* A Pathologic Cascade Leading to Synaptic Dysfunction in  $\alpha$ -Synuclein-Induced Neurodegeneration. *J. Neurosci.* **30**, 8083–8095 (2010).
132. Sun, J. *et al.* Functional cooperation of  $\alpha$ -synuclein and VAMP2 in synaptic vesicle recycling. *Proc. Natl. Acad. Sci. U. S. A.* **116**, 11113–11115 (2019).
133. Wang, L. *et al.*  $\alpha$ -synuclein multimers cluster synaptic-vesicles and attenuate recycling. *Curr. Biol. CB* **24**, 2319–2326 (2014).
134. Chandra, S., Gallardo, G., Fernández-Chacón, R., Schlüter, O. M. & Südhof, T. C.  $\alpha$ -Synuclein Cooperates with CSP $\alpha$  in Preventing Neurodegeneration. *Cell* **123**, 383–396 (2005).
135. Greten-Harrison, B. *et al.*  $\alpha\beta\gamma$ -Synuclein triple knockout mice reveal age-dependent neuronal dysfunction. *Proc. Natl. Acad. Sci.* **107**, 19573–19578 (2010).
136. Garcia-Reitböck, P. *et al.* SNARE protein redistribution and synaptic failure in a transgenic mouse model of Parkinson's disease. *Brain* **133**, 2032–2044 (2010).
137. Abeliovich, A. *et al.* Mice Lacking  $\alpha$ -Synuclein Display Functional Deficits in the Nigrostriatal Dopamine System. *Neuron* **25**, 239–252 (2000).
138. Senior, S. L. *et al.* Increased striatal dopamine release and hyperdopaminergic-like behaviour in mice lacking both alpha-synuclein and gamma-synuclein. *Eur. J. Neurosci.* **27**, 947–957 (2008).
139. Larsen, K. E. *et al.*  $\alpha$ -Synuclein Overexpression in PC12 and Chromaffin Cells Impairs Catecholamine Release by Interfering with a Late Step in Exocytosis. *J. Neurosci.* **26**, 11915–11922 (2006).
140. Mosharov, E. V. *et al.*  $\alpha$ -Synuclein Overexpression Increases Cytosolic Catecholamine Concentration. *J. Neurosci.* **26**, 9304–9311 (2006).
141. Gaugler, M. N. *et al.* Nigrostriatal overabundance of  $\alpha$ -synuclein leads to decreased vesicle density and deficits in dopamine release that correlate with reduced motor activity. *Acta Neuropathol. (Berl.)* **123**, 653–669 (2012).

142. Butler, B., Sambo, D. & Khoshbouei, H. Alpha-synuclein modulates dopamine neurotransmission. *J. Chem. Neuroanat.* **83–84**, 41–49 (2017).
143. Perez, R. G. *et al.* A Role for  $\alpha$ -Synuclein in the Regulation of Dopamine Biosynthesis. *J. Neurosci.* **22**, 3090–3099 (2002).
144. Peng, X. M.  $\alpha$ -Synuclein activation of protein phosphatase 2A reduces tyrosine hydroxylase phosphorylation in dopaminergic cells. *J. Cell Sci.* **118**, 3523–3530 (2005).
145. Chu, Y. & Kordower, J. H. Age-associated increases of  $\alpha$ -synuclein in monkeys and humans are associated with nigrostriatal dopamine depletion: Is this the target for Parkinson's disease? *Neurobiol. Dis.* **25**, 134–149 (2007).
146. Guo, J. T. *et al.* Inhibition of Vesicular Monoamine Transporter-2 Activity in  $\alpha$ -Synuclein Stably Transfected SH-SY5Y Cells. *Cell. Mol. Neurobiol.* **28**, 35–47 (2008).
147. Yamamoto, S., Fukae, J., Mori, H., Mizuno, Y. & Hattori, N. Positive immunoreactivity for vesicular monoamine transporter 2 in Lewy bodies and Lewy neurites in substantia nigra. *Neurosci. Lett.* **396**, 187–191 (2006).
148. Amara, S. G., Sanders, M. S., Zahniser, N. R., Povlock, S. L. & Daniels, G. M. Molecular Physiology and Regulation of Catecholamine Transporters. in *Advances in Pharmacology* (eds. Goldstein, D. S., Eisenhofer, G. & McCarty, R.) vol. 42 164–168 (Academic Press, 1997).
149. Butler, B. *et al.* Dopamine Transporter Activity Is Modulated by  $\alpha$ -Synuclein. *J. Biol. Chem.* **290**, 29542–29554 (2015).
150. Lee, F. J. S., Liu, F., Pristupa, Z. B. & Niznik, H. B. Direct binding and functional coupling of  $\alpha$ -synuclein to the dopamine transporters accelerate dopamine-induced apoptosis. *FASEB J.* **15**, 916–926 (2001).
151. Graham, D. R. & Sidhu, A. Mice Expressing the A53T Mutant Form of Human Alpha-Synuclein Exhibit Hyperactivity and Reduced Anxiety-Like Behavior. *J. Neurosci. Res.* **88**, 1777–1783 (2010).
152. Swant, J. *et al.*  $\alpha$ -Synuclein Stimulates a Dopamine Transporter-dependent Chloride Current and Modulates the Activity of the Transporter. *J. Biol. Chem.* **286**, 43933–43943 (2011).
153. Uversky, V. N. *et al.* Biophysical Properties of the Synucleins and Their Propensities to Fibrillate: INHIBITION OF  $\alpha$ -SYNUCLEIN ASSEMBLY BY  $\beta$ - AND  $\gamma$ -SYNUCLEINS. *J. Biol. Chem.* **277**, 11970–11978 (2002).
154. Bartels, T., Choi, J. G. & Selkoe, D. J.  $\alpha$ -Synuclein occurs physiologically as a helically folded tetramer that resists aggregation. *Nature* **477**, 107–110 (2011).
155. Wang, W. *et al.* A soluble  $\alpha$ -synuclein construct forms a dynamic tetramer. *Proc. Natl. Acad. Sci.* **108**, 17797–17802 (2011).
156. Burré, J. *et al.* Properties of Native Brain  $\alpha$ -Synuclein. *Nature* **498**, E4–E7 (2013).
157. Fauvet, B. *et al.*  $\alpha$ -Synuclein in Central Nervous System and from Erythrocytes, Mammalian Cells, and Escherichia coli Exists Predominantly as Disordered Monomer. *J. Biol. Chem.* **287**, 15345–15364 (2012).
158. Rovere, M., Sanderson, J. B., Fonseca-Ornelas, L., Patel, D. S. & Bartels, T. Refolding of helical soluble  $\alpha$ -synuclein through transient interaction with lipid interfaces. *FEBS Lett.* **592**, 1464–1472 (2018).
159. Kayed, R., Dettmer, U. & Lesné, S. E. Soluble endogenous oligomeric  $\alpha$ -synuclein species in neurodegenerative diseases: Expression, spreading, and cross-talk. *J. Park. Dis.* **Preprint**, 1–28 (2020).

160. Uversky, V. N. A Protein-Chameleon: Conformational Plasticity of  $\alpha$ -Synuclein, a Disordered Protein Involved in Neurodegenerative Disorders. *J. Biomol. Struct. Dyn.* **21**, 211–234 (2003).
161. Ghosh, D. *et al.* Structure based aggregation studies reveal the presence of helix-rich intermediate during  $\alpha$ -Synuclein aggregation. *Sci. Rep.* **5**, 9228 (2015).
162. Vilar, M. *et al.* The fold of  $\alpha$ -synuclein fibrils. *Proc. Natl. Acad. Sci. U. S. A.* **105**, 8637–8642 (2008).
163. Ghosh, D., Mehra, S., Sahay, S., Singh, P. K. & Maji, S. K.  $\alpha$ -synuclein aggregation and its modulation. *Int. J. Biol. Macromol.* **100**, 37–54 (2017).
164. Bengoa-Vergniory, N., Roberts, R. F., Wade-Martins, R. & Alegre-Abarategui, J. Alpha-synuclein oligomers: a new hope. *Acta Neuropathol. (Berl.)* **134**, 819–838 (2017).
165. Caughey, B. & Lansbury, P. T. P ROTOFIBRILS , P ORES , F IBRILS, AND N EURODEGENERATION : Separating the Responsible Protein Aggregates from The Innocent Bystanders. *Annu. Rev. Neurosci.* **26**, 267–298 (2003).
166. Andreasen, M., Lorenzen, N. & Otzen, D. Interactions between misfolded protein oligomers and membranes: A central topic in neurodegenerative diseases? *Biochim. Biophys. Acta BBA - Biomembr.* **1848**, 1897–1907 (2015).
167. Fagerqvist, T. *et al.* Off-pathway  $\alpha$ -synuclein oligomers seem to alter  $\alpha$ -synuclein turnover in a cell model but lack seeding capability in vivo. *Amyloid Int. J. Exp. Clin. Investig. Off. J. Int. Soc. Amyloidosis* **20**, 233–244 (2013).
168. Näsström, T. *et al.* The lipid peroxidation products 4-oxo-2-nonenal and 4-hydroxy-2-nonenal promote the formation of  $\alpha$ -synuclein oligomers with distinct biochemical, morphological, and functional properties. *Free Radic. Biol. Med.* **50**, 428–437 (2011).
169. Pieri, L., Madiona, K. & Melki, R. Structural and functional properties of prefibrillar  $\alpha$ -synuclein oligomers. *Sci. Rep.* **6**, (2016).
170. Lashuel, H. A. *et al.*  $\alpha$ -Synuclein, Especially the Parkinson's Disease-associated Mutants, Forms Pore-like Annular and Tubular Protofibrils. *J. Mol. Biol.* **322**, 1089–1102 (2002).
171. Volles, M. J. & Lansbury, P. T. Zeroing in on the Pathogenic Form of  $\alpha$ -Synuclein and Its Mechanism of Neurotoxicity in Parkinson's Disease †. *Biochemistry* **42**, 7871–7878 (2003).
172. Chinta, S. J., Mallajosyula, J. K., Rane, A. & Andersen, J. K. Mitochondrial  $\alpha$ -synuclein accumulation impairs complex I function in dopaminergic neurons and results in increased mitophagy in vivo. *Neurosci. Lett.* **486**, 235–239 (2010).
173. Luth, E. S., Stavrovskaya, I. G., Bartels, T., Kristal, B. S. & Selkoe, D. J. Soluble, prefibrillar  $\alpha$ -synuclein oligomers promote complex I-dependent, Ca<sup>2+</sup>-induced mitochondrial dysfunction. *J. Biol. Chem.* **289**, 21490–21507 (2014).
174. Colla, E. *et al.* Accumulation of toxic  $\alpha$ -synuclein oligomer within endoplasmic reticulum occurs in  $\alpha$ -synucleinopathy in vivo. *J. Neurosci. Off. J. Soc. Neurosci.* **32**, 3301–3305 (2012).
175. Fusco, G. *et al.* Structural basis of membrane disruption and cellular toxicity by  $\alpha$ -synuclein oligomers. *Science* **358**, 1440–1443 (2017).
176. Danzer, K. M. *et al.* Different Species of  $\alpha$ -Synuclein Oligomers Induce Calcium Influx and Seeding. *J. Neurosci.* **27**, 9220–9232 (2007).
177. Kim, C. *et al.* Neuron-released oligomeric  $\alpha$ -synuclein is an endogenous agonist of TLR2 for paracrine activation of microglia. *Nat. Commun.* **4**, 1562 (2013).

178. Hoffmann, A.-C. *et al.* Extracellular aggregated alpha synuclein primarily triggers lysosomal dysfunction in neural cells prevented by trehalose. *Sci. Rep.* **9**, 544 (2019).
179. Schulz-Schaeffer, W. J. The synaptic pathology of  $\alpha$ -synuclein aggregation in dementia with Lewy bodies, Parkinson's disease and Parkinson's disease dementia. *Acta Neuropathol. (Berl.)* **120**, 131–143 (2010).
180. Outeiro, T. F. *et al.* Formation of Toxic Oligomeric  $\alpha$ -Synuclein Species in Living Cells. *PLoS ONE* **3**, (2008).
181. Helwig, M. *et al.* Brain propagation of transduced  $\alpha$ -synuclein involves non-fibrillar protein species and is enhanced in  $\alpha$ -synuclein null mice. *Brain* **139**, 856–870 (2016).
182. Behere, A. *et al.* Visualization of early oligomeric  $\alpha$ -synuclein pathology and its impact on the dopaminergic system in the (Thy-1)-h[A30P] $\alpha$ -syn transgenic mouse model. *J. Neurosci. Res.* **99**, 2525–2539 (2021).
183. Roberts, R. F., Wade-Martins, R. & Alegre-Abarrategui, J. Direct visualization of alpha-synuclein oligomers reveals previously undetected pathology in Parkinson's disease brain. *Brain J. Neurol.* **138**, 1642–1657 (2015).
184. Sekiya, H. *et al.* Wide distribution of alpha-synuclein oligomers in multiple system atrophy brain detected by proximity ligation. *Acta Neuropathol. (Berl.)* **137**, 455–466 (2019).
185. Cremades, N. *et al.* Direct Observation of the Interconversion of Normal and Toxic Forms of  $\alpha$ -Synuclein. *Cell* **149**, 1048–1059 (2012).
186. Chen, S. W. *et al.* Structural characterization of toxic oligomers that are kinetically trapped during  $\alpha$ -synuclein fibril formation. *Proc. Natl. Acad. Sci. U. S. A.* **112**, E1994–E2003 (2015).
187. Froula, J. M. *et al.* Defining  $\alpha$ -synuclein species responsible for Parkinson's disease phenotypes in mice. *J. Biol. Chem.* **294**, 10392–10406 (2019).
188. Buell, A. K. *et al.* Solution conditions determine the relative importance of nucleation and growth processes in  $\alpha$ -synuclein aggregation. *Proc. Natl. Acad. Sci.* **111**, 7671–7676 (2014).
189. Luk, K. C. *et al.* Exogenous  $\alpha$ -synuclein fibrils seed the formation of Lewy body-like intracellular inclusions in cultured cells. *Proc. Natl. Acad. Sci.* **106**, 20051–20056 (2009).
190. Luk, K. C., Kehm, V., Carroll, J., Zhang, B. & Trojanowski, J. Q. Pathological  $\alpha$ -Synuclein Transmission Initiates Parkinson-like Neurodegeneration in Non-transgenic Mice. **338**, 5 (2012).
191. Shimosawa, A. *et al.* Propagation of pathological  $\alpha$ -synuclein in marmoset brain. *Acta Neuropathol. Commun.* **5**, 12 (2017).
192. Chu, Y. *et al.* Intrastratial alpha-synuclein fibrils in monkeys: spreading, imaging and neuropathological changes. *Brain* **142**, 3565–3579 (2019).
193. Bousset, L. *et al.* Structural and functional characterization of two alpha-synuclein strains. *Nat. Commun.* **4**, (2013).
194. Peelaerts, W. *et al.*  $\alpha$ -Synuclein strains cause distinct synucleinopathies after local and systemic administration. *Nature* **522**, 340–344 (2015).
195. Guo, J. L. *et al.* Distinct  $\alpha$ -Synuclein Strains Differentially Promote Tau Inclusions in Neurons. *Cell* **154**, (2013).
196. Lau, A. *et al.*  $\alpha$ -Synuclein Strains Target Distinct Brain Regions and Cell Types. *Nat. Neurosci.* **23**, 21–31 (2020).

197. Sajjani, G. & Requena, J. R. Prions, proteinase K and infectivity. *Prion* **6**, 430–432 (2012).
198. Neumann, M. *et al.* Misfolded proteinase K-resistant hyperphosphorylated alpha-synuclein in aged transgenic mice with locomotor deterioration and in human alpha-synucleinopathies. *J. Clin. Invest.* **110**, 1429–1439 (2002).
199. Neumann, M., Müller, V., Kretzschmar, H. A., Haass, C. & Kahle, P. J. Regional distribution of proteinase K-resistant alpha-synuclein correlates with Lewy body disease stage. *J. Neuropathol. Exp. Neurol.* **63**, 1225–1235 (2004).
200. Tanji, K. *et al.* Proteinase K-resistant  $\alpha$ -synuclein is deposited in presynapses in human Lewy body disease and A53T  $\alpha$ -synuclein transgenic mice. *Acta Neuropathol. (Berl.)* **120**, 145–154 (2010).
201. Giasson, B. I., Murray, I. V. J., Trojanowski, J. Q. & Lee, V. M.-Y. A Hydrophobic Stretch of 12 Amino Acid Residues in the Middle of  $\alpha$ -Synuclein Is Essential for Filament Assembly. *J. Biol. Chem.* **276**, 2380–2386 (2001).
202. Miake, H., Mizusawa, H., Iwatsubo, T. & Hasegawa, M. Biochemical Characterization of the Core Structure of  $\alpha$ -Synuclein Filaments. *J. Biol. Chem.* **277**, 19213–19219 (2002).
203. Abd-Elhadi, S. *et al.* Total and Proteinase K-Resistant  $\alpha$ -Synuclein Levels in Erythrocytes, Determined by their Ability to Bind Phospholipids, Associate with Parkinson's Disease. *Sci. Rep.* **5**, (2015).
204. Holdorff, B. Friedrich Heinrich Lewy (1885-1950) and his work. *J. Hist. Neurosci.* **11**, 19–28 (2002).
205. Kosaka, K. Lewy bodies in cerebral cortex. Report of three cases. *Acta Neuropathol. (Berl.)* **42**, 127–134 (1978).
206. Shahmoradian, S. H. *et al.* Lewy pathology in Parkinson's disease consists of crowded organelles and lipid membranes. *Nat. Neurosci.* **22**, 1099–1109 (2019).
207. Moors, T. E. *et al.* The subcellular arrangement of alpha-synuclein proteoforms in the Parkinson's disease brain as revealed by multicolor STED microscopy. *Acta Neuropathol. (Berl.)* **142**, 423–448 (2021).
208. Manzanza, N. de O., Sedlackova, L. & Kalaria, R. N. Alpha-Synuclein Post-translational Modifications: Implications for Pathogenesis of Lewy Body Disorders. *Front. Aging Neurosci.* **13**, 690293 (2021).
209. Oueslati, A. Implication of Alpha-Synuclein Phosphorylation at S129 in Synucleinopathies: What Have We Learned in the Last Decade? *J. Park. Dis.* **6**, 39–51.
210. Fujiwara, H. *et al.*  $\alpha$ -Synuclein is phosphorylated in synucleinopathy lesions. *Nat. Cell Biol.* **4**, 160–164 (2002).
211. Ghanem, S. S. *et al.*  $\alpha$ -Synuclein phosphorylation at serine 129 occurs after initial protein deposition and inhibits seeded fibril formation and toxicity. *Proc. Natl. Acad. Sci.* **119**, e2109617119 (2022).
212. Mahul-Mellier, A.-L. *et al.* The process of Lewy body formation, rather than simply  $\alpha$ -synuclein fibrillization, is one of the major drivers of neurodegeneration. *Proc. Natl. Acad. Sci.* **117**, 4971–4982 (2020).
213. Braak, H., Rüb, U., Gai, W. P. & Del Tredici, K. Idiopathic Parkinson's disease: possible routes by which vulnerable neuronal types may be subject to neuroinvasion by an unknown pathogen. *J. Neural Transm.* **110**, 517–536 (2003).
214. Li, J.-Y. *et al.* Lewy bodies in grafted neurons in subjects with Parkinson's disease suggest host-to-graft disease propagation. *Nat. Med.* **14**, 501–503 (2008).

215. El-Agnaf, O. M. A. *et al.* Alpha-synuclein implicated in Parkinson's disease is present in extracellular biological fluids, including human plasma. *FASEB J. Off. Publ. Fed. Am. Soc. Exp. Biol.* **17**, 1945–1947 (2003).
216. Mao, X. *et al.* Pathological  $\alpha$ -synuclein transmission initiated by binding lymphocyte-activation gene 3. *Science* **353**, aah3374 (2016).
217. Shrivastava, A. N. *et al.*  $\alpha$ -synuclein assemblies sequester neuronal  $\alpha 3$ -Na<sup>+</sup>/K<sup>+</sup>-ATPase and impair Na<sup>+</sup> gradient. *EMBO J.* **34**, 2408–2423 (2015).
218. Holmes, B. B. *et al.* Heparan sulfate proteoglycans mediate internalization and propagation of specific proteopathic seeds. *Proc. Natl. Acad. Sci. U. S. A.* **110**, E3138-3147 (2013).
219. Ihse, E. *et al.* Cellular internalization of alpha-synuclein aggregates by cell surface heparan sulfate depends on aggregate conformation and cell type. *Sci. Rep.* **7**, 9008 (2017).
220. Polinski, N. K. *et al.* Best Practices for Generating and Using Alpha-Synuclein Pre-Formed Fibrils to Model Parkinson's Disease in Rodents. *J. Park. Dis.* **8**, 303–322 (2018).
221. Birol, M., Wojcik, S. P., Miranker, A. D. & Rhoades, E. Identification of N-linked glycans as specific mediators of neuronal uptake of acetylated  $\alpha$ -Synuclein. *PLoS Biol.* **17**, e3000318 (2019).
222. Peelaerts, W. *et al.*  $\alpha$ -Synuclein strains cause distinct synucleinopathies after local and systemic administration. *Nature* **522**, 340–344 (2015).
223. Lancaster, G. I. & Febbraio, M. A. Exosome-dependent trafficking of HSP70: a novel secretory pathway for cellular stress proteins. *J. Biol. Chem.* **280**, 23349–23355 (2005).
224. Gibbins, D. J., Ciaudo, C., Erhardt, M. & Voinnet, O. Multivesicular bodies associate with components of miRNA effector complexes and modulate miRNA activity. *Nat. Cell Biol.* **11**, 1143–1149 (2009).
225. Danzer, K. M. *et al.* Exosomal cell-to-cell transmission of alpha synuclein oligomers. *Mol. Neurodegener.* **7**, 42 (2012).
226. Alvarez-Erviti, L. *et al.* Lysosomal dysfunction increases exosome-mediated alpha-synuclein release and transmission. *Neurobiol. Dis.* **42**, 360–367 (2011).
227. Tairarol, L. *et al.* The 3.0 Cell Communication: New Insights in the Usefulness of Tunneling Nanotubes for Glioblastoma Treatment. *Cancers* **13**, 4001 (2021).
228. Abounit, S. *et al.* Tunneling nanotubes spread fibrillar  $\alpha$ -synuclein by intercellular trafficking of lysosomes. *EMBO J.* **35**, 2120–2138 (2016).
229. Dieriks, B. V. *et al.*  $\alpha$ -synuclein transfer through tunneling nanotubes occurs in SH-SY5Y cells and primary brain pericytes from Parkinson's disease patients. *Sci. Rep.* **7**, 42984 (2017).
230. Rostami, J. *et al.* Human Astrocytes Transfer Aggregated Alpha-Synuclein via Tunneling Nanotubes. *J. Neurosci.* **37**, 11835–11853 (2017).
231. Rajasekaran, S. & Witt, S. N. Trojan horses and tunneling nanotubes enable  $\alpha$ -synuclein pathology to spread in Parkinson disease. *PLoS Biol.* **19**, e3001331 (2021).
232. Giguère, N., Burke Nanni, S. & Trudeau, L.-E. On Cell Loss and Selective Vulnerability of Neuronal Populations in Parkinson's Disease. *Front. Neurol.* **9**, (2018).
233. Hijaz, B. A. & Volpicelli-Daley, L. A. Initiation and propagation of  $\alpha$ -synuclein aggregation in the nervous system. *Mol. Neurodegener.* **15**, 19 (2020).

234. Taguchi, K., Watanabe, Y., Tsujimura, A. & Tanaka, M. Expression of  $\alpha$ -synuclein is regulated in a neuronal cell type-dependent manner. *Anat. Sci. Int.* **94**, 11–22 (2019).
235. Luna, E. *et al.* Differential  $\alpha$ -synuclein expression contributes to selective vulnerability of hippocampal neuron subpopulations to fibril-induced toxicity. *Acta Neuropathol. (Berl.)* **135**, 855–875 (2018).
236. Cao, Y.-L. *et al.* A role of BAG3 in regulating SNCA/ $\alpha$ -synuclein clearance via selective macroautophagy. *Neurobiol. Aging* **60**, 104–115 (2017).
237. Streit, W. J., Walter, S. A. & Pennell, N. A. Reactive microgliosis. *Prog. Neurobiol.* **57**, 563–581 (1999).
238. Lai, T. T. *et al.* Temporal Evolution of Inflammation and Neurodegeneration With Alpha-Synuclein Propagation in Parkinson’s Disease Mouse Model. *Front. Integr. Neurosci.* **15**, (2021).
239. Duffy, M. F. *et al.* Lewy body-like alpha-synuclein inclusions trigger reactive microgliosis prior to nigral degeneration. *J. Neuroinflammation* **15**, (2018).
240. Imamura, K. *et al.* Distribution of major histocompatibility complex class II-positive microglia and cytokine profile of Parkinson’s disease brains. *Acta Neuropathol. (Berl.)* **106**, 518–526 (2003).
241. Gerhard, A. *et al.* In vivo imaging of microglial activation with [11C](R)-PK11195 PET in idiopathic Parkinson’s disease. *Neurobiol. Dis.* **21**, 404–412 (2006).
242. Hughes, C. D. *et al.* Picomolar concentrations of oligomeric alpha-synuclein sensitizes TLR4 to play an initiating role in Parkinson’s disease pathogenesis. *Acta Neuropathol. (Berl.)* **137**, 103–120 (2019).
243. Wang, S. *et al.*  $\alpha$ -Synuclein, a chemoattractant, directs microglial migration via H<sub>2</sub>O<sub>2</sub>-dependent Lyn phosphorylation. *Proc. Natl. Acad. Sci.* **112**, E1926–E1935 (2015).
244. Hou, L. *et al.* Integrin CD11b mediates  $\alpha$ -synuclein-induced activation of NADPH oxidase through a Rho-dependent pathway. *Redox Biol.* **14**, 600–608 (2018).
245. Harms, A. S., Ferreira, S. A. & Romero-Ramos, M. Periphery and brain, innate and adaptive immunity in Parkinson’s disease. *Acta Neuropathol. (Berl.)* **141**, 527–545 (2021).
246. Wang, W. *et al.* Caspase-1 causes truncation and aggregation of the Parkinson’s disease-associated protein  $\alpha$ -synuclein. *Proc. Natl. Acad. Sci. U. S. A.* **113**, 9587–9592 (2016).
247. Rostami, J. *et al.* Astrocytes have the capacity to act as antigen-presenting cells in the Parkinson’s disease brain. *J. Neuroinflammation* **17**, 119 (2020).
248. Yun, S. P. *et al.* Block of A1 astrocyte conversion by microglia is neuroprotective in models of Parkinson’s disease. *Nat. Med.* **24**, 931–938 (2018).
249. Chavarría, C., Rodríguez-Bottero, S., Quijano, C., Cassina, P. & Souza, J. M. Impact of monomeric, oligomeric and fibrillar alpha-synuclein on astrocyte reactivity and toxicity to neurons. *Biochem. J.* **475**, 3153–3169 (2018).
250. Borghammer, P. & Van Den Berge, N. Brain-First versus Gut-First Parkinson’s Disease: A Hypothesis. *J. Park. Dis.* **9**, S281–S295 (2019).
251. Uemura, N. *et al.* Inoculation of  $\alpha$ -synuclein preformed fibrils into the mouse gastrointestinal tract induces Lewy body-like aggregates in the brainstem via the vagus nerve. *Mol. Neurodegener.* **13**, 21 (2018).

252. Brochard, V. *et al.* Infiltration of CD4<sup>+</sup> lymphocytes into the brain contributes to neurodegeneration in a mouse model of Parkinson disease. *J. Clin. Invest.* **119**, 182–192 (2009).
253. Harms, A. S. *et al.*  $\alpha$ -Synuclein fibrils recruit peripheral immune cells in the rat brain prior to neurodegeneration. *Acta Neuropathol. Commun.* **5**, 85 (2017).
254. Pey, P., Pearce, R. K. B., Kalaitzakis, M. E., Griffin, W. S. T. & Gentleman, S. M. Phenotypic profile of alternative activation marker CD163 is different in Alzheimer's and Parkinson's disease. *Acta Neuropathol. Commun.* **2**, 21 (2014).
255. Williams-Gray, C. H. *et al.* Serum immune markers and disease progression in an incident Parkinson's disease cohort (ICICLE-PD). *Mov. Disord.* **31**, 995–1003 (2016).
256. Sulzer, D. *et al.* T cells from patients with Parkinson's disease recognize  $\alpha$ -synuclein peptides. *Nature* **546**, 656–661 (2017).
257. Lindestam Arlehamn, C. S. *et al.*  $\alpha$ -Synuclein-specific T cell reactivity is associated with preclinical and early Parkinson's disease. *Nat. Commun.* **11**, 1875 (2020).
258. Santaella, A. *et al.* Inflammation biomarker discovery in Parkinson's disease and atypical parkinsonisms. *BMC Neurol.* **20**, 26 (2020).
259. Blandini, F. & Armentero, M.-T. Animal models of Parkinson's disease. *FEBS J.* **279**, 1156–1166 (2012).
260. Chesselet, M.-F. In vivo alpha-synuclein overexpression in rodents: a useful model of Parkinson's disease? *Exp. Neurol.* **209**, 22–27 (2008).
261. Duffy, M. F. *et al.* Quality Over Quantity: Advantages of Using Alpha-Synuclein Preformed Fibril Triggered Synucleinopathy to Model Idiopathic Parkinson's Disease. *Front. Neurosci.* **12**, (2018).
262. Recasens, A., Ulusoy, A., Kahle, P. J., Di Monte, D. A. & Dehay, B. In vivo models of alpha-synuclein transmission and propagation. *Cell Tissue Res.* **373**, 183–193 (2018).
263. Polinski, N. K. A Summary of Phenotypes Observed in the In Vivo Rodent Alpha-Synuclein Preformed Fibril Model. *J. Park. Dis.* **11**, 1555–1567.
264. Patterson, J. R. *et al.* Generation of Alpha-Synuclein Preformed Fibrils from Monomers and Use In Vivo. *JoVE J. Vis. Exp.* e59758 (2019) doi:10.3791/59758.
265. Landeck, N. *et al.* Stereotaxic Intracranial Delivery of Chemicals, Proteins or Viral Vectors to Study Parkinson's Disease. *JoVE J. Vis. Exp.* e62128 (2021) doi:10.3791/62128.
266. Söderberg, O. *et al.* Direct observation of individual endogenous protein complexes in situ by proximity ligation. *Nat. Methods* **3**, 995–1000 (2006).
267. Dettmer, U. & Bartels, T. ExPLAining early synucleinopathies. *Brain* **138**, 1449–1451 (2015).
268. Williams-Gray, C. Seeing Is Believing: Alpha-Synuclein Oligomers in Parkinson's Disease Brain. *Mov. Disord.* **30**, 1324–1324 (2015).
269. Hernández, L. F. An A-PLAuse to a new assay that unveils previously undetected alpha-synucleinopathies. *Mov. Disord.* **31**, 301–301 (2016).
270. Ruffmann, C. *et al.* Detection of alpha-synuclein conformational variants from gastro-intestinal biopsy tissue as a potential biomarker for Parkinson's disease. *Neuropathol. Appl. Neurobiol.* **44**, 722–736 (2018).
271. Mazzetti, S. *et al.*  $\alpha$ -Synuclein oligomers in skin biopsy of idiopathic and monozygotic twin patients with Parkinson's disease. *Brain* **143**, 920–931 (2020).

272. O'Hara, D. M., Kalia, S. K. & Kalia, L. V. Methods for detecting toxic  $\alpha$ -synuclein species as a biomarker for Parkinson's disease. *Crit. Rev. Clin. Lab. Sci.* **57**, 291–307 (2020).
273. Raykova, D. *et al.* A method for Boolean analysis of protein interactions at a molecular level. *Nat. Commun.* **13**, 4755 (2022).
274. Koos, B. *et al.* Proximity-dependent initiation of hybridization chain reaction. *Nat. Commun.* **6**, 7294 (2015).
275. Klaesson, A. *et al.* Improved efficiency of in situ protein analysis by proximity ligation using UnFold probes. *Sci. Rep.* **8**, 5400 (2018).
276. Kumar, S. T. *et al.* How specific are the conformation-specific  $\alpha$ -synuclein antibodies? Characterization and validation of 16  $\alpha$ -synuclein conformation-specific antibodies using well-characterized preparations of  $\alpha$ -synuclein monomers, fibrils and oligomers with distinct structures and morphology. *Neurobiol. Dis.* **146**, 105086 (2020).
277. Roberts, R. F., Bengoa-Vergniory, N. & Alegre-Abarategui, J. Alpha-Synuclein Proximity Ligation Assay (AS-PLA) in Brain Sections to Probe for Alpha-Synuclein Oligomers. *Methods Mol. Biol. Clifton NJ* **1948**, 69–76 (2019).
278. Kahle, P. J. *et al.* Subcellular Localization of Wild-Type and Parkinson's Disease-Associated Mutant  $\alpha$ -Synuclein in Human and Transgenic Mouse Brain. *J. Neurosci.* **20**, 6365–6373 (2000).
279. Freichel, C. *et al.* Age-dependent cognitive decline and amygdala pathology in alpha-synuclein transgenic mice. *Neurobiol. Aging* **28**, 1421–1435 (2007).
280. Fagerqvist, T. *et al.* Monoclonal antibodies selective for  $\alpha$ -synuclein oligomers/protofibrils recognize brain pathology in Lewy body disorders and  $\alpha$ -synuclein transgenic mice with the disease-causing A30P mutation. *J. Neurochem.* **126**, 131–144 (2013).
281. Lassen, L. B. *et al.* ELISA method to detect  $\alpha$ -synuclein oligomers in cell and animal models. *PLOS ONE* **13**, e0196056 (2018).
282. Ekmark-Lewén, S. *et al.* Early fine motor impairment and behavioral dysfunction in (Thy-1)-h[A30P] alpha-synuclein mice. *Brain Behav.* **8**, e00915 (2018).
283. Schell, H., Hasegawa, T., Neumann, M. & Kahle, P. J. Nuclear and neuritic distribution of serine-129 phosphorylated  $\alpha$ -synuclein in transgenic mice. *Neuroscience* **160**, 796–804 (2009).
284. Almandoz-Gil, L. *et al.* Mapping of Surface-Exposed Epitopes of In Vitro and In Vivo Aggregated Species of Alpha-Synuclein. *Cell. Mol. Neurobiol.* **37**, 1217–1226 (2017).
285. Bengoa-Vergniory, N. *et al.* Tau-proximity ligation assay reveals extensive previously undetected pathology prior to neurofibrillary tangles in preclinical Alzheimer's disease. *Acta Neuropathol. Commun.* **9**, 18 (2021).

# Acta Universitatis Upsaliensis

*Digital Comprehensive Summaries of Uppsala Dissertations  
from the Faculty of Medicine 1866*

Editor: The Dean of the Faculty of Medicine

A doctoral dissertation from the Faculty of Medicine, Uppsala University, is usually a summary of a number of papers. A few copies of the complete dissertation are kept at major Swedish research libraries, while the summary alone is distributed internationally through the series Digital Comprehensive Summaries of Uppsala Dissertations from the Faculty of Medicine. (Prior to January, 2005, the series was published under the title “Comprehensive Summaries of Uppsala Dissertations from the Faculty of Medicine”.)

Distribution: [publications.uu.se](http://publications.uu.se)  
urn:nbn:se:uu:diva-482999



ACTA  
UNIVERSITATIS  
UPSALIENSIS  
UPPSALA  
2022